PAPER

Check for updates

Emission time and amount of crop residue burning play critical role on PM$_{2.5}$ variability during October–November in northwestern India during 2022–2024

Akash Biswal, [†*a] Masayuki Takigawa, [b] Poonam Mangaraj, [‡a] Jagat S. H. Bisht, [§b] Prabir K. Patra, [*ab] Yutaka Matsumi, [ac] Tomoki Nakayama, [ad] Hikaru Araki,[a] Natsuko Yasutomi, [¶a] Vikas Singh [e] and the Aakash CUPI-G team‖

High incidences of crop residue burning (CRB) in Punjab and Haryana during October–November is one of the major causes of elevated PM$_{2.5}$ in Delhi National Capital Region (NCR). An estimation of precise contribution of CRB emissions to PM$_{2.5}$ levels in Delhi-NCR is hindered by uncertainties in meteorology, atmospheric chemistry and emissions, and lack of quality observations. We use continuous *in situ* observations of PM$_{2.5}$ from a wide area network of 30 stations during 16 October to 30 November (peak CRB season) of 2022, 2023 and 2024 under Aakash project. The WRF-Chem model is used for simulation of chemical compositions of the atmosphere over the northwest India region. We have incorporated five distinct CRB emission scenarios in addition to commonly used industrial and biological emissions for the simulations. Scenarios with and without CRB emissions from different regions were compared to assess their impacts on PM$_{2.5}$. The average CRB emission impact on PM$_{2.5}$ concentrations in Delhi-NCR during CRB season are estimated at 18%, 16% and 9% in 2022, 2023 and 2024, respectively. The low impact of CRB on PM$_{2.5}$ in 2024 could arise from a shift in CRB time to evening, which was not captured by existing emission inventories due to absence of satellite overpass in late evening. A shift to late evening CRB leads to very strong nighttime build-up of PM$_{2.5}$ due to emissions when the boundary layer is shallow. Inclusion of appropriate diurnal and synoptic variability in CRB emissions is important for simulating observed PM$_{2.5}$ levels and evaluation human health exposures.

Environmental significance

Using continuous observations at 30 sites and WRF-chem model simulations the impact of crop residue burning (CRB) emission on PM$_{2.5}$ over northwestern India is studied. CRB emission shows a decreasing trend over Punjab and Haryana, due to which, the contribution of CRB to Delhi PM$_{2.5}$ was reduced dramatically from 18% and 16% in 2022 and 2023, respectively, to 9% in 2024. However, the observed PM$_{2.5}$ from CUPI-G network shows continuously high PM$_{2.5}$ over the rural sites of Punjab, evidently highlighting the limitation of our understanding the air pollution in the region. For instance, incorporating missing biomass burning emission on cloudy/hazy days improves model performance and similarly when a shift in peak CRB activities is adopted from 2:30 pm local time to 6:30 pm the model performance is substantially improved. The diurnal profile of CRB emission must be carefully accounted in the global/regional emission inventories by improving fire count/area detection.

aResearch Institute for Humanity and Nature (RIHN), Kyoto, Japan. E-mail: akashbiswal800@gmail.com; prabir@chikyu.ac.jp

bResearch Institute for Global Change, JAMSTEC, Yokohama, Japan. E-mail: prabir@jamstec.go.jp

cNagoya University, Nagoya, Japan

dNagasaki University, Nagasaki, Japan

eCommission for Air Quality Management (CAQM), New Delhi, Delhi 110001, India

† Now at University of Surrey, Guildford, United Kingdom.

‡ Now at Sustainable Futures Collaborative, New Delhi, India.

§ Now at National Institute for Environmental Studies (NIES), Tsukuba, Japan.

¶ Now at Yukawa Institute for Theoretical Physics, Kyoto University, Kyoto, Japan.

‖ A full list of team authors appears in Section 5.

1 Introduction

Air pollution poses a serious threat to human health, with 99% of the global population living below the standards set by the World Health Organization.[1] An estimate suggests air pollution is responsible for approximately 4.72 (3.48–5.80) million deaths worldwide, with India alone accounting for around 1.9 (1.6–2.3) millions of these fatalities.[2] Among all cities, Delhi stands out as the most polluted; consistently maintaining an annual average concentration over 100 μg m^{-3}, albeit with a gradual decline due to recent policy interventions, except for 2024.[3–6] The

© 2025 The Author(s). Published by the Royal Society of Chemistry

Environ. Sci.: Atmos., 2025, 5, 1211–1229 | 1211

magnitude of $PM_{2.5}$ concentration in Delhi exhibits seasonal variation, influenced by a complex interplay of local emissions sources, meteorological conditions and transport of pollution from external domains.[3–5,7,8] Crop residue burning (CRB) emissions is one of the major problems for the northwest Indian states, which could account for more than 50% share for $PM_{2.5}$ on episode scales during the October–November months.[9–16]

The post-monsoon months (October–November) have heightened pollution levels in Delhi region, attributed to factors such as lower boundary layer height, atmospheric stagnation due to temperature inversion, increased small-scale burning for domestic heating, and emissions from CRB in neighboring states.[11,17–19] This period coincides with the harvesting season of kharif rice and land clearing for following crop season, which exert additional pollutant emissions at higher intensity because kharif rice harvesting is delayed due to the Preservation of Subsoil Water Act enacted in 2009.[20,21] Higher population density in Delhi-NCR, downwind from the CRB emission regions of Punjab elevates the exposure level, thereby contributing to adverse health effects among the population.[22,23] It is now well known that the $PM_{2.5}$ formed out of CRB particularly have high oxidative potential by Patel et al.[24] which would enhance the health-related exposure to the rural population in Punjab where very high $PM_{2.5}$ (exceeding 500 μg m^{-3}) is observed lasting more than a couple of weeks in November.[19,25,26]

The contribution of CRB to air pollution in northwest India during October–November has been extensively investigated through various modeling studies and only recently using low-cost in situ sensor measurements, including the rural agricultural areas.[18,19,27] This low-cost sensor network is deployed by the Aakash project at RIHN, Kyoto and provided crucial information on $PM_{2.5}$ variability and captured continuous evaluation of the emissions from CRB (https://aakash-rihn.org/en/data-set/).[28] It has been established that the Compact and Useful $PM_{2.5}$ Instruments with Gas sensors (CUPI-Gs) perform well when efficiently monitored at the beginning of the deployment in September, operational period and at the end of the deployment in March of Aakash Project's main campaign periods in 2022–2023, 2023–2024 and 2024–2025. The CUPI-G performances have been checked at laboratory conditions (un published data), measurements from nearby sites at JNU and US Embassy[18,19] or co-located measurements.[29]

The emissions from CRB are generally estimated using fuel load data derived from satellite-observed fire detection counts (FDC) and burned area,[30,31] along with emission factors specific to cropland.[32,33] The CRB emissions show considerable variation across different global fire emission products using standard burned area and FDC which fails to observe during some days.[30,31] These uncertainties in fire detection products are influenced by various factors, including satellite transit time and cloud cover, which can obstruct fire detection as well as the proxies of high emission activities, such as the pollutant concentrations.[18,34] Liu et al. estimated the emission increase of tenfold from 70 to 800 Gg when accounting for missing fires due to satellite detection limitations.[35] However, the CRB emissions beyond the satellite transit hours is under explored and

currently missing in the global fire emission datasets, and we show here that quality-controlled continuous measurements by the low-cost CUPI-G sensor network can help overcome some of the deficiencies in remote sensing measurements due to spatio-temporal data gaps.

The present study addresses critical gaps in understanding CRB contributions by evaluating the performance of the WRF-Chem model under various emission scenarios for 2022, 2023 and 2024, with particular focus on emission timing and amount. In addition to traditional CRB scenarios, factors identified as crucial based on the limitations in the available global emission datasets. We specifically designed scenarios to overcome two major challenges: (1) the predominance of evening-time fire emissions that often occur after satellite overpass times, and (2) the reduced detection of fire activities during cloudy days. These scenarios likely explain the challenges associated to estimate CRB emission contributions to regional $PM_{2.5}$ levels. Our evaluation incorporates comparison with high-resolution data from the CUPI-G sensors collected throughout Punjab, Haryana and Delhi-NCR.[18,19] By simulating these specific emission timing and quantity scenarios, we aim to provide an assessment of CRB contribution to overall $PM_{2.5}$ levels in northwestern India during 2022–2024, when sharpest fall in the satellite observed FDC and burned area are reported in Punjab or Haryana (Fig. S1), and increases in $PM_{2.5}$ are observed on the ground from Punjab through Delhi (this study; Roychowdhury and Kaur[6]).

2 Model, data and methods

2.1 WRF-Chem model configuration

We use WRF-Chem version 3.9.1.1 to perform the chemistry-transport model (CTM) simulation experiments. Fig. 1a depicts the topographic map, with mean sea level elevation ranging from 0 to 8000 meters, and the two domains of model simulation. The map highlights the complex topography of the Himalayan region. The WRF-Chem model's nested domain setup is overlaid, with the outer domain (D01) covering a wide area at a 27×27 km^2 resolution and the inner domain (D02) focusing on a smaller region at a 9×9 km^2 horizonal resolution (Fig. 1a). Our model setup consists of 41 vertical layers, with lowest layer thickness of 22 m and about 14 model layers below 2 km. The intricate terrain of the Himalayas, with its steep elevation changes, significantly affects local meteorological and atmospheric conditions, requiring precise modeling configuration. Fig. 1b depicts the Land Use Land Cover (LULC) map, using a product from European Space Application Center (ESA), where the predominant light-green areas denote cropland. This map also shows example locations of CUPI-G measurement sites (black dots) of the AAKASH project.[28]

We used the European Centre for Medium-Range Weather Forecasts (ECMWF) Reanalysis v5 (ERA5) data at a horizontal resolution of $0.25° \times 0.25°$ for initializing the meteorology and supply boundary conditions to WRF.[36] Four-dimensional data assimilation (FDDA) applied through grid nudging. Nudging was conducted for horizontal winds, temperature, and humidity at 60 minute intervals both within and above the planetary
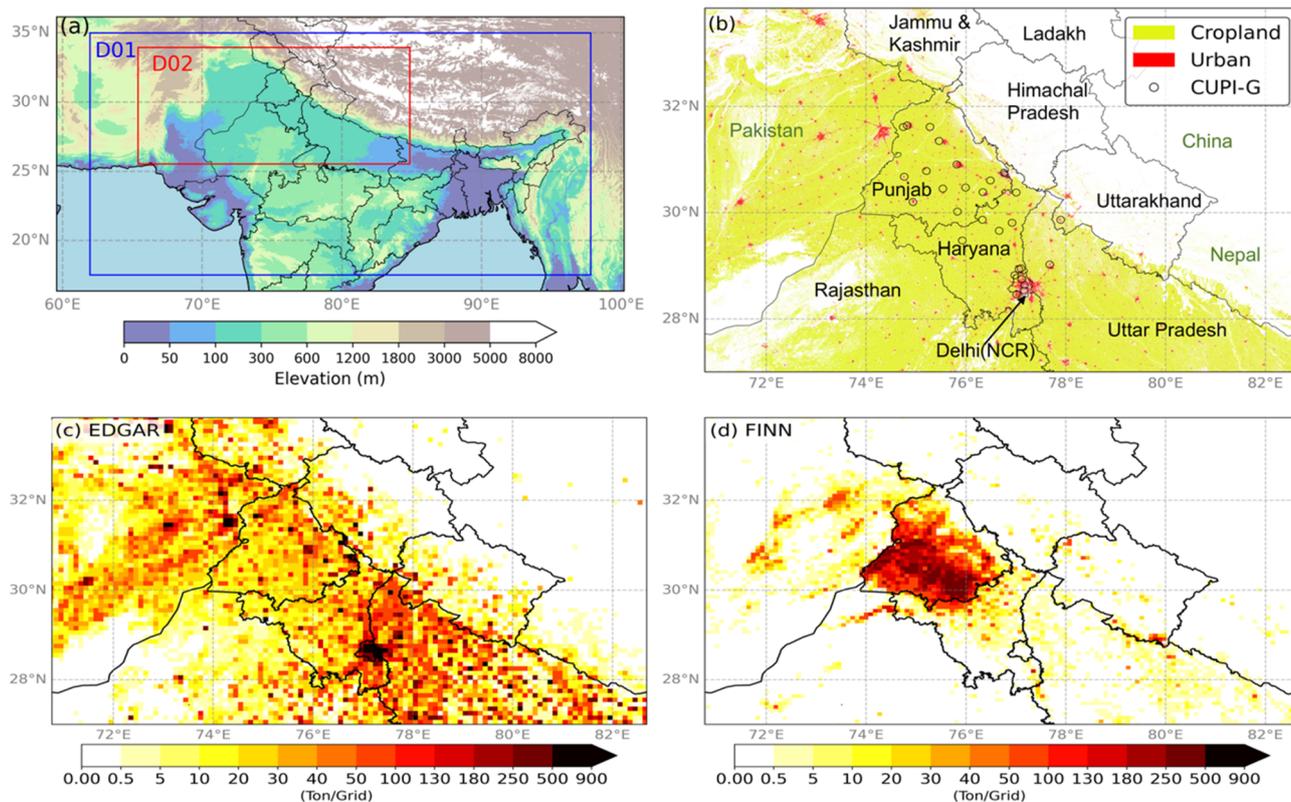
Fig. 1 (a) Map of WRF-Chem model domains with the terrain height (source: https://iridl.ldeo.columbia.edu/SOURCES/.NOAA/.NGDC/.GLOBE/.topo/data.nc), and (b) the spread of 2024 CUPI-G sensor network over two major LULC types (yellowish-green for agricultural land, red is for urban area; source: European Space Agency (ESA) WorldCover, version 2, https://esa-worldcover.org/en). Also shown are the distributions of EDGAR anthropogenic/industrial emission of PM$_{2.5}$ (c) and FINN-v2.5 biomass burning for the same geographical area for 2022 (d). FINN open biomass burning emissions represent mainly the crop residue burning in October–November months. Indian administrative shapefile is obtained from https://surveyofindia.gov.in/pages/political-map-of-india. The names of Indian states are marked on panel b (text in black), along with neighbouring countries (in green coloured text).

boundary layer, which is shown to produce realistic meteorology over the India region.[37] The Copernicus Atmosphere Monitoring Service (CAMS) global reanalysis dataset was used to provide chemical initial and boundary conditions for WRF-Chem simulations. The WRF-Chem simulation was initialized with a spin-up period of 7 days prior to the analysis window to allow for chemical and meteorological fields to stabilize. The simulation results from D02 are used in the analysis and are believed to be sufficient for resolving the observed gradients between sites in our observation network, considering that (1) the site-to-site distances are mostly greater than 9 km (Fig. 1b), and (2) PM$_{2.5}$ has residence time longer than several days during most days (except for the rain washout events) of October–November in the region.

The model uses RACM gas-phase chemistry linked to the Goddard Chemistry Aerosol Radiation and Transport (GOCART) aerosol scheme (RACM-GOCART). The GOCART aerosol model simulates five major types of aerosols, namely, sulfate, black carbon, organic carbon, dust, and sea salt. Nitrate and secondary organic aerosols from gas to particle are missing in the used scheme. The chemical aerosol scheme GOCART does not include the secondary gas to particle formation, and likely underestimate background PM$_{2.5}$ concentration in the

region.[38,39] However, this has been used by number of studies for research and operational air pollution forecast system to study the transport of regional emissions.[38] The planetary boundary layer (PBL) scheme used in the model setting is Shin–Hong scale-aware scheme (bl_pbl_physics = 11).[40] This grid-scale-aware scheme can handle the subgrid-scale (SGS) turbulent transport at sub-kilometer grid resolution by including the effect of the grid-size on the non-local transport profile.[40] The performance of this scheme for simulating PBL height, relative humidity and wind speed has close agreement with the observation over the India domain.[41]

2.2 Emission datasets

2.2.1 Biogenic emissions. Biogenic emissions were simulated online by the Model of Emissions of Gases and Aerosols from Nature (MEGAN).[42] Major biogenic species are isoprene, hydrocarbons (C2-CX), myrcene and sabinene *etc.*

2.2.2 Anthropogenic emissions. Anthropogenic emissions are based on the Emission Database for Global Atmospheric Research, version 6.1 (EDGAR-v6.1) global emission inventory for the year 2018, at 0.1° × 0.1° horizontal resolution.[43,44] SI Fig. S2 shows the spatial distributions of total anthropogenic/

© 2025 The Author(s). Published by the Royal Society of Chemistry

Environ. Sci.: Atmos., 2025, **5**, 1211–1229 | **1213**

Table 1 Anthropogenic/industrial and open biomass burning emissions of PM$_{2.5}$ for November (Gg per month). Since the FINN-v2.5 (final product) was not available at the time of our model simulations, FINN near real-time (NRT) emissions are used for 2024. The open biomass burning emissions, as derived from satellite fire products, mostly arise from CRB

Dataset	Sector/region	Punjab	Haryana	NCR	Delhi	Uttar Pradesh
EDGAR v6.1	Chemical processes	0.02	0.02	0.05	0.02	0.17
	Power industry	2.81	1.04	2.98	0.85	11.91
	Industrial combustion	2.09	0.57	2.85	1.17	11.81
	Residential	3.06	0.83	2.61	0.10	8.65
	Traffic road dust resuspension	0.03	0.01	0.05	0.01	0.09
	Traffic exhaust	0.08	0.03	0.13	0.02	0.22
FINN-v2.5	CRB/BB 2022	43	2.8	—	—	2.9
FINN-v2.5	CRB/BB 2023	41.6	1.8	—	—	3
FINN-NRT	CRB/BB 2024	16.9	1.7	—	—	9.4

industrial emissions are shown for four key pollutants: PM$_{2.5}$, and carbon monoxide (CO), NO$_x$, and non-methane volatile organic compounds (NMVOCs). High emission grids are concentrated around urban and industrial regions, particularly in the Delhi-NCR region. The emissions vary from 3 to 5880, 0.9 to 1700 and 0.5 to 970 for CO, NO$_x$ and NMVOC, respectively. These emission maps highlight the spatial variability and intensity of different pollutants over the densely populated/ urban areas and industrialized areas for CO, PM$_{2.5}$ and NMVOC. Table 1 shows the state wise PM$_{2.5}$ emissions for the month of November over Punjab, Haryana, Delhi, Delhi-NCR districts, Haryana, and Uttar Pradesh. The emissions per unit

area over Delhi and surrounding NCR districts are high in magnitude compared with the other administrative districts.

2.2.3 FINN fire emission. The open biomass burning is derived from the Fire Inventory from NCAR (FINN, versions 2.5, NRT).[30,31] The emissions are based on satellite-measured locations of active fires and emission factors relevant to the underlying land cover.[32] The FINN-v2.5 (final product) fire emissions are available at 1 km spatial and hourly temporal resolution (**https://www.acom.ucar.edu/Data/fire/**, last access: 13 May 2024). The FINN-NRT are available in near real time (NRT) and using the input of MODIS NRT fire counts. The FINN-v2.5, which incorporates enhanced satellite detection
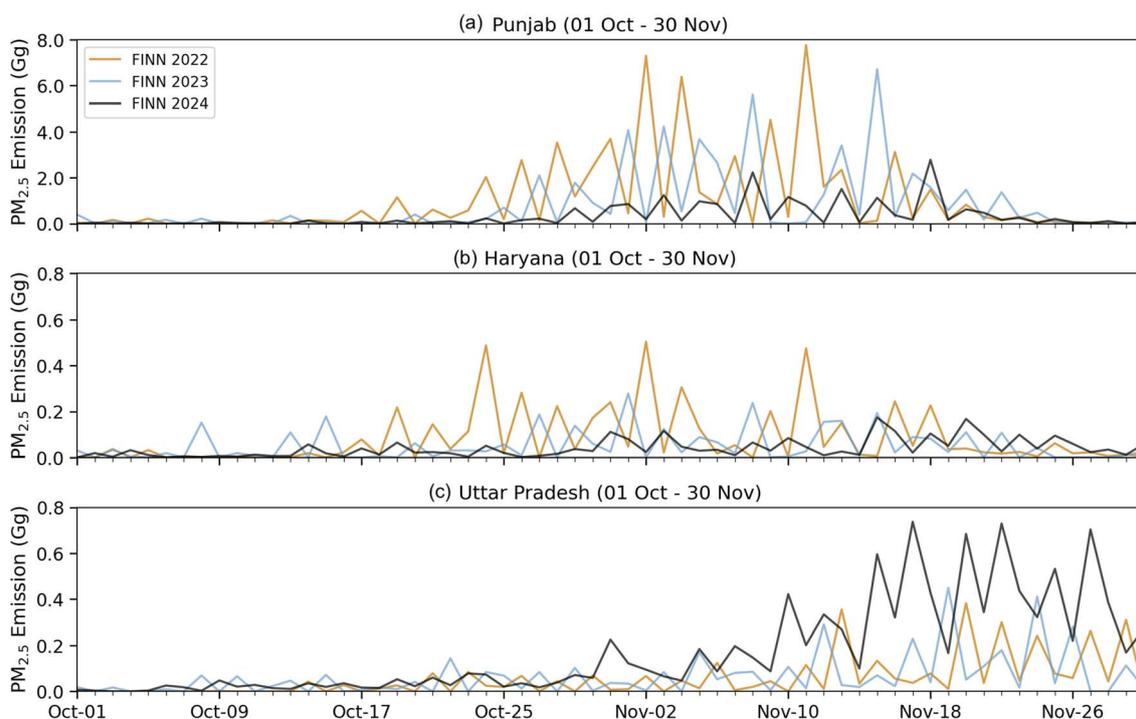
Fig. 2 Evolution of regionally aggregated FINN PM$_{2.5}$ emissions in October and November months over the administrative regions of 3 northwest Indian states as a whole ((a) Punjab, (b) Haryana, (c) Uttar Pradesh) and different colours show emissions for year 2022 and 2023 (version 2.5), and 2024 (version NRT). Note that the y-axis range for the top panel (Punjab emissions) is an order of magnitude greater than those for the lower two panels.

algorithms and considers MODIS + VIIRS shows a higher magnitude of fire emission estimates compared to FINN-NRT.[31]

The magnitude of fire emissions is highest for the southern part of Punjab followed by six-fold lower than the northern part of Punjab, entire state of Haryana and Uttar Pradesh. The temporal evolution of biomass burning (BB) emission for three states are shown in Fig. 2 for FINN emission data products. The BB emissions over Punjab and Haryana has a decreasing pattern from 2022 to 2024, however, the BB emission over Uttar Pradesh shows an increasing pattern which is more prominent in the later part of the month of November. We have used fire emissions from FINN-v2.5 for 2022 and 2023, and FINN-NRT for the year 2024. The 2024 emissions are found to be drastically lower than the previous 2 years for Punjab and Haryana (Fig. 2), and this issue is discussed further in the results section.

2.3 Model sensitivity cases to emissions of biomass burning

Emissions due to CRB/BB are one of the most uncertain components in the region of our study while comparing model simulations with measurements. Emissions from different inventories and prior to posterior emissions due to CRB can vary up to an order of magnitude.[27,35] The uncertainty in CRB emission can arise from cloud cover or shifted time of burning (sometimes to avoid satellite surveillance; ref. various media articles), assumed emission factor and fuel load *etc.* To test some of these hypotheses and their effect on simulated $PM_{2.5}$, we have run the following 4 sensitivity simulations, in addition to the WRF-CTL case:

(1) WRF-CTL: control case, includes all the emission sectors as mentioned above (Fig. S3a). The FINN biomass burning emissions are supplied to WRF-Chem with an idealized diurnal cycle that peaks at 2 pm (20% emissions in 1 hour) and has a trough at midnight (10% emissions in 1 hour).

(2) WRF-NoBB: excludes biomass burning emissions as a whole, compared to the WRF-CTL case (Fig. S3b).

(3) WRF-PUBB: only include biomass burning emissions exclusively from the state of Punjab to isolate the effect of Punjab emissions (Fig. S3c).

(4) WRF-missBB: involves an emission filling approximation during the cloud cover days or hazy days where FINN could not produce any emission due to lack of fire count or burnt area detection (Fig. S4).[18] Details are given in Table 2, following analysis of daily emissions (Fig. S5).

(5) WRF-EvBB: this scenario considers the practice of farmers resorting to burn crop residues in the late afternoon, to avoid detection by satellites which overpasses at 10:30 IST (MODIS) or 13:30 IST (Suomi NPP/NOAA-20), which was majorly identified by the local authorities in the year 2024. We have shifted the peak of usual diurnal emission by four hours ensuring the total daily emission value for each pixel remains conserved (as depicted in Fig. S6).

2.4 Calculation of BB contribution to $PM_{2.5}$

One of the important questions faced by the policymakers is the sectoral contributions to the increase in $PM_{2.5}$ in the October–November months in Delhi-NCR, particularly from the CRB activities. Share of biomass burning emissions to the $PM_{2.5}$ concentrations at each of the CUPI-G site is calculated as:

$$\text{BB share } (\%) = \left(\frac{\text{WRF-CTL} - \text{WRF-NoBB}}{\text{WRF-CTL}}\right) \times 100 \quad (1)$$

Table 2 Various emission scenarios for Biomass Burning (BB) sensitivity assessment. List of the WRF-Chem model simulations cases are given for the control (CTL) and 4 sensitivity cases

Emission scenarios used in WRF-Chem simulations

Model cases	Anthropogenic	Natural	Biomass burning (BB)	Detailed note
WRF-CTL	EDGAR, version 6.1	MEGAN + GOCART	FINN (v2.5/NRT, MODIS)	BB over all grids in respective domains; peak emission occurs at 2:30 pm local time (IST) on each grid
WRF-NoBB			NA	BB emissions excluded
WRF-PUBB			FINN (v2.5, MODIS)	BB only on grids in the state of Punjab, India
WRF-missBB (accounting for the cloud cover days)			FINN (v2.5, MODIS) + hypothetical missing emissions	November 11 emissions used for November 3–10 across all grids for 2022 November 5 emissions used for November 2–12 across all grids for 2023 This simulation was not run for 2024
WRF-EvBB (shifting behaviour)			FINN (NRT, MODIS)	Peak emission time is shifted to 6:30 pm local time for 2022 and 2024 This simulation was not run for 2023

© 2025 The Author(s). Published by the Royal Society of Chemistry

Environ. Sci.: Atmos., 2025, **5**, 1211–1229 | **1215**

where WRF-CTL the control simulation case using all emissions and WRF-NoBB case excluded biomass burning emissions. This calculation is performed using simulations for the innermost domain, D02, with a 9 km spatial resolution. By comparing scenarios with and without biomass burning emissions, the BB share (%) isolates the specific contribution of crop residue burning to $PM_{2.5}$ levels. We provide regional contributions by averaging over several sites in 4 region divisions over our study area.

2.5 *In situ* surface observation from CUPI-G stations

The CUPI-G field campaign was held in 2022, 2023 and 2024 during the month of September–November covering the intense crop residue burning events over the states of Punjab and Haryana, and transport to the neighbouring regions (Fig. 3). Overlapping dots in the map indicate the existence of common and different observation sites across multiple years. CUPI-G is a low-cost sensor, affordable to monitor air pollutant concentrations at reasonable accuracy (approx. ±10%) to study air pollution in the region.[18,19,45] More details related to field campaign and associated results are available elsewhere.[18,19] The details, such as the development and performance reliability of the low-cost $PM_{2.5}$ sensors were presented by Nakayama *et al.*[45] The observation networks were divided into four categories based on the CRB emission specific geographical regions as North Punjab, Southwest Punjab, Central Haryana and Delhi-NCR (Fig. 3).[19] However, not all the sites are
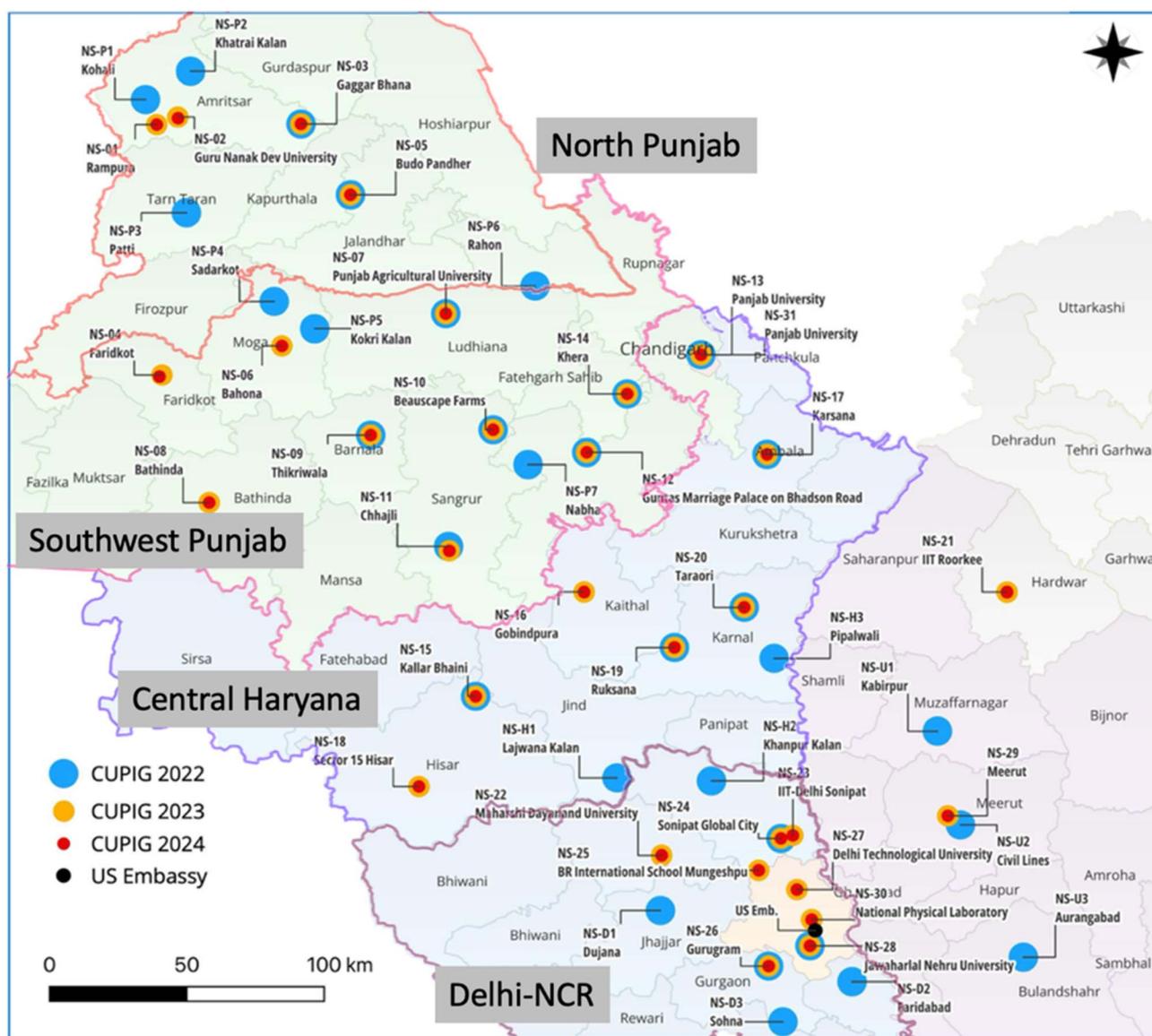

Fig. 3 Spatial distribution of the CUPI-G observation network across northwest India. The coloured dots represent the observation sites for a specific year (ref. legends). The black dot represents the location of the US-Embassy standard instrument in New Delhi. For analysis of time series data and presenting in this work, we have grouped the CUPI-G sites to represent 4 regions of our study area as marked by coloured lines, and identified by region names the text in grey background.
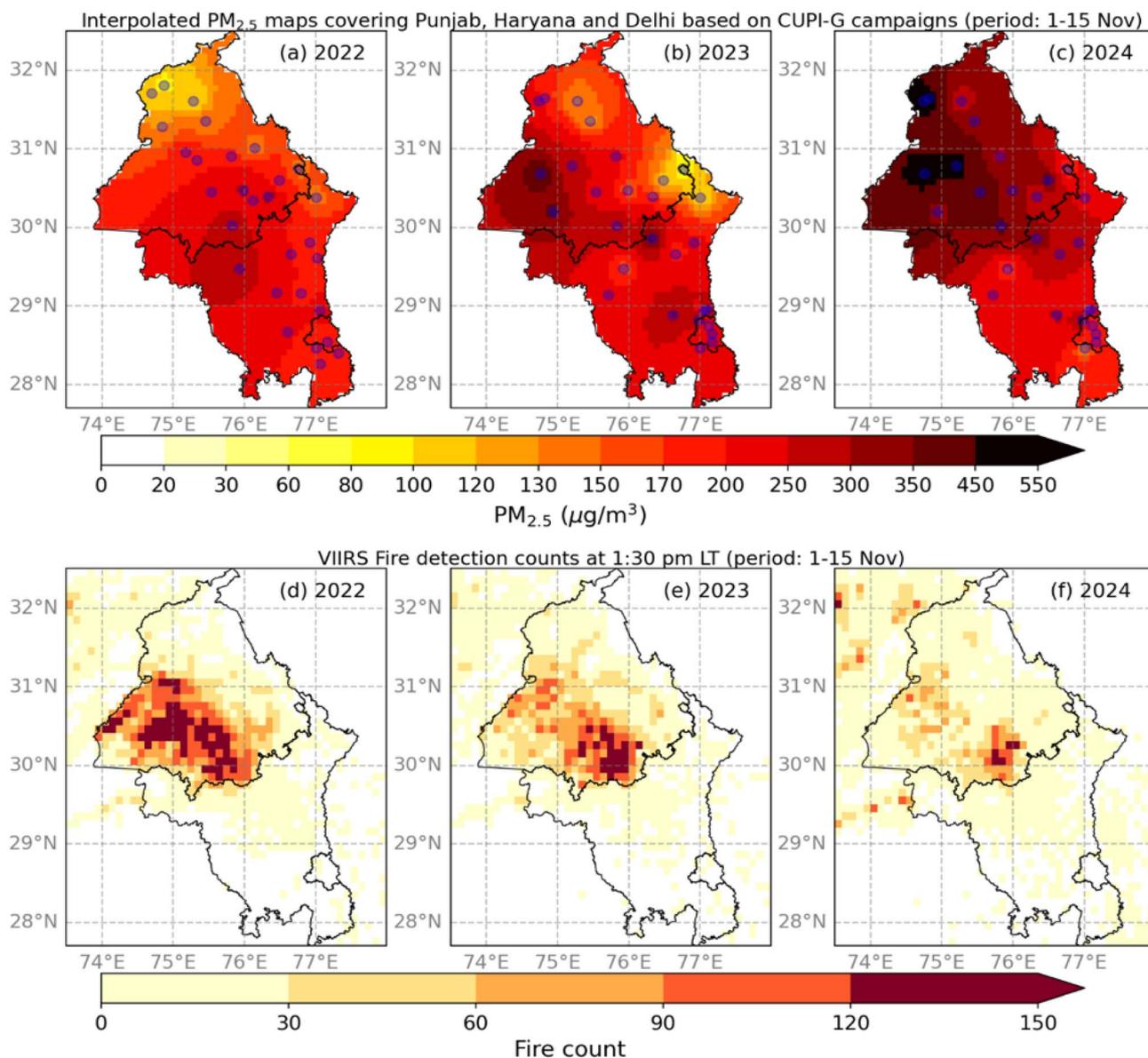
1216 | *Environ. Sci.: Atmos.*, 2025, **5**, 1211–1229

© 2025 The Author(s). Published by the Royal Society of Chemistry

Fig. 4 Spatial distribution of CUPI-G PM$_{2.5}$ concentration for 1–15 November-mean for (a) 2022, (b) 2023 and (c) 2024. The blue dots represent the CUPI-G station location for each year of campaign. VIIRS fire count at 10 km spatial resolution for (d) 2022, (e) 2023 and (f) 2024. An animation of PM$_{2.5}$ and FDC maps at daily time intervals is provided in the SI document (Animation 1). The VIIRS FDCs were obtained from NASA FIRMS (https://firms.modaps.eosdis.nasa.gov/) and gridded to 0.1° × 0.1° spatial resolution.

used in averaging regional mean PM$_{2.5}$ values, except for the sites with less than a few days of data gaps within one month (ref. Table S2 for details).

2.6 Spatial map from CUPI-G measurements at the site network

Observations from spatially derived CUPI-G PM$_{2.5}$ concentration at 9 km resolution over the regions of Punjab, Haryana and Delhi. A geospatial interpolation technique: Inverse Distance Weighting (IDW) has been used in preparation of spatial PM$_{2.5}$ plots, which is a deterministic interpolation method and an in-built spatial analyst tool available in ArcGIS software version 10.8.1. It uses a linearly weighted combination of sample points

to determine cell (grid) values with weight inversely proportional to distance. It assigns higher weights to points closer to the target location, where the weights are being determined as an inverse function of the distance raised to the power of 'p' (a positive real number). Higher values of 'p' increase the influence of nearby points on the interpolation. The predicted value at the target location is computed by summing the products of the assigned weights and the measured values from all points. For this study, the parameter 'p' is set to 2 based on a review of existing literature.[46,47]

The spatial concentration maps of PM$_{2.5}$ for three years at 9 km spatial resolution, based on CUPI-G observed location data (Fig. 3), have been generated with averaged PM$_{2.5}$ for 1–15

© 2025 The Author(s). Published by the Royal Society of Chemistry

Environ. Sci.: Atmos., 2025, 5, 1211–1229 | 1217

November as shown in Fig. 4a–c. The $PM_{2.5}$ concentration over the southwest region of Punjab exceeded 300 μg m^{-3}, making it the most polluted in all three years and aligns well with the FINN emission inventory (Fig. 1d) indicating a similitude between CRB emissions (FINN) and air quality (CUPI-G $PM_{2.5}$). In Delhi, average $PM_{2.5}$ concentrations consistently range between 200–250 μg m^{-3} in all three years. The spatial distributions of $PM_{2.5}$ in the CRB region are more representative in 2023 and 2024 due to an improved placement of monitoring sites for capturing the CRB emission signals. The locations of CUPI-G sites in 2022 did not cover the lower half of the Punjab and Haryana states (Fig. 4a), and missed to capture the origin and transport of high CRB plumes from the southwestern Punjab, as evident from the VIIRS fire count map (Fig. 4d).

To have a one-to-one comparison with the concentration maps based on CUPI-G data, similar interpolated maps are also prepared for each model cases. This is done by sampling the model results at the CUPI-G sites for the respective years hourly intervals and then applied the identical methodology as discussed above. Discussions of these comparisons and results are given Section 3.2. Such map creation from site-based observations is known as objective analysis and widely applied for meteorological weather analysis.[48]

3   Results

3.1   Evaluation of simulated $PM_{2.5}$ over 4 regions using measurements

The concentration of $PM_{2.5}$ is affected by the complex interplay of anthropogenic emissions, BB emissions and atmospheric processes of secondary particle formation, dilution and dispersion. The performance of model simulation is evaluated using $PM_{2.5}$ concentrations at daily intervals over the four regions of North Punjab, Southwest Punjab, Central Haryana and Delhi-NCR (Table 2) and shown as scatter plot in Fig. S7a–c. In North Punjab where the CRB typically occurs early in the season, during mid-late October, the model fit to the observations is relatively weak, with correlation coefficient (r) in the range of 0.35 to 0.58, indicating a moderate model performance in capturing $PM_{2.5}$ variability (Table 3). Southwest Punjab with the highest CRB emission exhibits a moderate fit with r-values ranging between 0.58 to 0.70, showing a similar slope but better correlation than that for North Punjab. Central Haryana also

shows moderate model performance, with r-values ranging from 0.3 to 0.5. The performance over Delhi-NCR, with r-values of 0.7 for 2022, 0.57 for 2023 and 0.07. The model performance over Delhi-NCR for 2024 is notably poor which potentially indicates the missing BB emissions over Punjab in 2024. Overall, the model underpredicts $PM_{2.5}$ levels consistently for all regions but performs relatively better in Delhi-NCR for 2022 and 2023 compared to the other areas. It is not clear if the underprediction is related to the GOCART chemical scheme, without the secondary aerosol formation, or the emission distribution and magnitude are inadequately estimated.

3.2   Spatial pattern of $PM_{2.5}$ concentration

Gridded maps of air pollutants based on observation are required for accurate assessment of various impacts, $e.g.$, human health, road and rail transport, aviation, and also assess applicability of model simulations for impact analyses. The spatial pattern of mean $PM_{2.5}$ concentrations from 1–15 November 2022 for 3 different emission scenarios are shown in Fig. 5 (ref. Fig. S8 and S9 for the cases as appropriate for 2023 and 2024, respectively). The gridded concentration at the lowest model level (Fig. 5a–c) and the interpolated map after sampling the model at the CUPI-G measurement sites (Fig. 4a) do not show the same features suggesting that the model maps and observation maps cannot be compared directly (Fig. 5a–c and 4a). However, the observed features of the spatial patterns begin to emerge, such as the highest concentration over the southwest Punjab, when the model is first extracted for the CUPI sites and interpolated maps are created, $i.e.$, WRF-"case"@CUPI (Fig. 5d–f). The differences between the model maps with and without sampling at CUPI-G sites are smaller for 2023 (Fig. S8) and 2024 (Fig. S9), compared to those for 2022, because of better placement of the sampling sites. Although interpolated, such creation of map by objective analysis can aid in understanding the movement and progression of short-lived air pollutants purely based on measurements, when the measurements are covering the study region with relatively uniform spatial coverage.

Fig. 5a shows the effect of biomass burning emissions over the Punjab region with higher $PM_{2.5}$ concentration of ∼140 μg m^{-3}, as simulated by WRF-CTL, and up to ∼120 μg m^{-3} over Haryana and Delhi-NCR. This difference in concentration gradient over the three states highlights the substantial impact

Table 3 Model $vs.$ observed $PM_{2.5}$ (unit: μg m^{-3}) comparison statistics for four different regions for October 16 to November 30 over all the years using data at daily intervals. Mean of observations (Mean_obs) and WRF-CTL model (Mean_mod), Pearson's correlation coefficient (r), mean model − observation bias (MB) and root mean-squared error (RMSE) are given

Region	Central Haryana			Delhi-NCR			North Punjab			Southwest Punjab		
	2022	2023	2024	2022	2023	2024	2022	2023	2024	2022	2023	2024
Obs	152	160	222	139	169	172	101	113	203	151	215	283
Model	93	98	85	87	109	91.3	86	86	89	106	119	92
R	0.55	0.52	0.35	0.73	0.57	0.07	0.35	0.56	0.58	0.58	0.65	0.7
MB	−59	−62	−137	−53	−60	−81	−15	−27	−114	−45	−95	−192
RMSE	87	89	177	71	92	156	47	52	137	97	131	251

of regional biomass burning, when compared with other anthropogenic sources over Delhi. However, while comparing WRF-CTL@CUPI (Fig. 5d) with the CUPI-G map (Fig. 4a), the modelled concentration of 2022 shows an underestimation, indicated by the statistics in Table 3. With the addition of missing-day emissions, WRF-missBB PM$_{2.5}$ in Fig. 5b and e improves the modelled concentration, better aligning with the spatial distribution of CUPI-G measured concentration (Fig. 4a). Remarkable improvements in agreement for the patterns of the observed (Fig. 4a) and WRF-EvBB (Fig. 5f), showing the high concentrations of modelled PM$_{2.5}$ (~200 µg m^{-3}) are extending until the Delhi-NCR. However, the WRF-EvBB simulation over-estimated PM$_{2.5}$ in the Punjab region, when compared with the observed.

In 2023, CUPI-G derived map has higher PM$_{2.5}$ compared to 2022 because of the prolonged CRB emission after the second week of November in 2023 (Fig. 4a and b). The WRF-missBB (Fig. S8d) case further improves the PM$_{2.5}$ and fits well with the spatial distribution in CUPI-G derived map (Fig. 4b). Similarly for 2024 the WRF-CTL highly underestimates the PM$_{2.5}$ across all the states due to very low emissions from CRB as estimated by FINN-NRT, while the measurement of CUPI-Gs showed highest PM$_{2.5}$ value among the 3 years. However, the simulated WRF-EvBB case produces PM$_{2.5}$ levels closer to observations, with a similar spatial distribution based on CUPI-G data (Fig. 4c), suggesting a shift in farmer's regular practice of early afternoon CRB to evening CRB. It is noted that the wetter crop residues (evening condition) produce greater emissions of
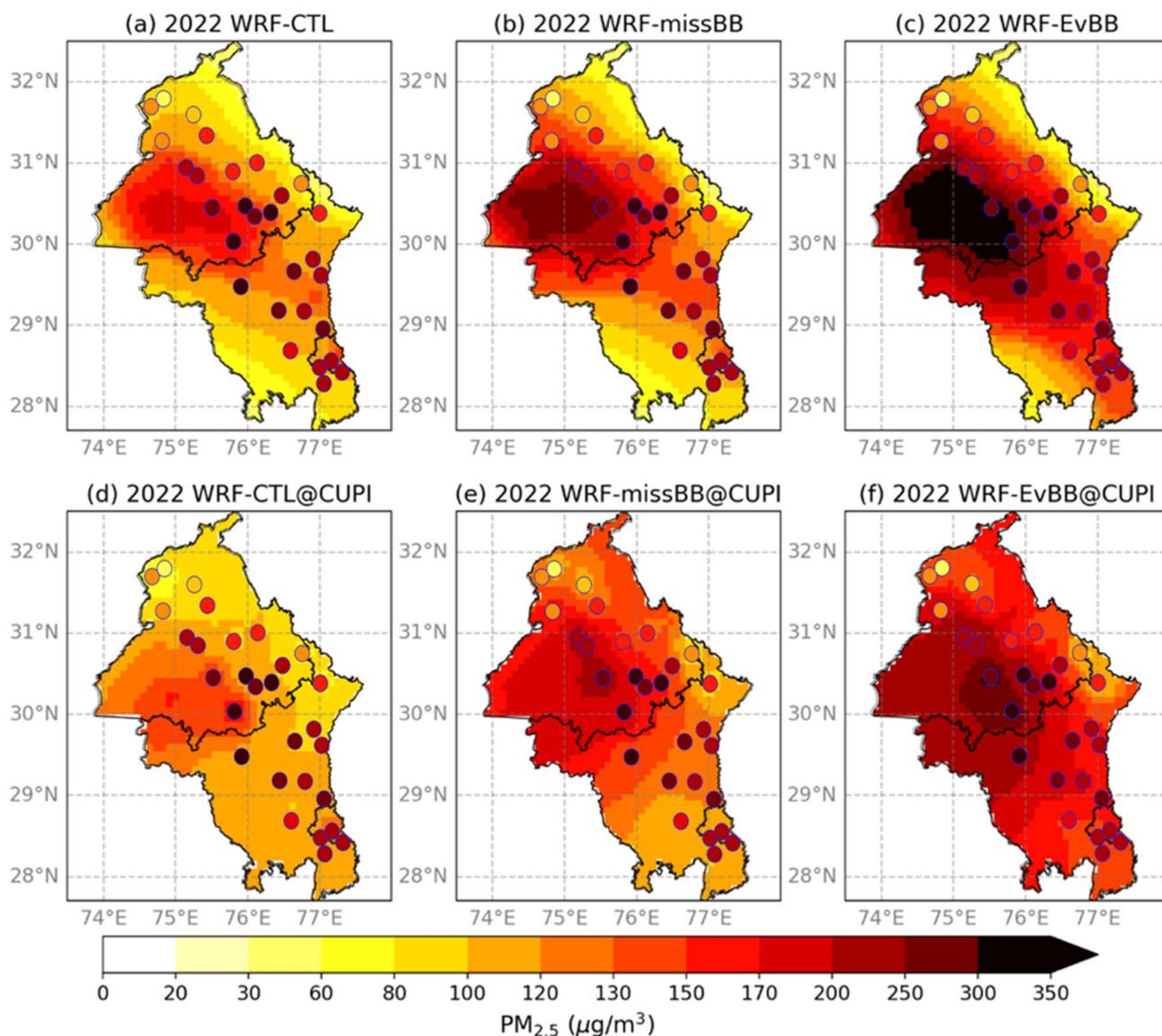

Fig. 5 Spatial distribution of 01–15 November-mean PM$_{2.5}$ concentration for 2022. Comparisons show WRF-Chem model simulations for various emission scenarios (top row), (a) WRF-CTL, (b) WRF-missBB, (c) WRF-EvBB, in comparison with CUPI-G based maps (bottom row) which are prepared after sampling the model results at the CUPI-G sites ((d) WRF-CTL@CUPI, (e) WRF-missBB@CUPI, (f) WRF-EvBB@CUPI). Colour inside the circle varies as per the mean observed concentration at the CUPI-G sites on the common colour bar. Similar map plots for simulations using a selected number of cases are shown in Fig. S8 and S9 for the years 2023 and 2024, respectively.

© 2025 The Author(s). Published by the Royal Society of Chemistry

Environ. Sci.: Atmos., 2025, **5**, 1211–1229 | **1219**

particulate and gaseous pollutants compared to drier residues (early afternoon condition).[49] Most research on emissions from CRB have focused on increasing the area burnt,[35] but estimation of variable emission factor under different conditions of the residues and soil underneath is less explored and not accounted for in the current major emission inventories (FINN, GFAS or GFED). The time series and statistical analysis of WRF-missBB and WRF-EvBB are detailed in Section 3.5.

3.3 Daily mean $PM_{2.5}$ from WRF-Chem *vs.* CUPI-G for four regions

Daily mean $PM_{2.5}$ concentrations measured by the CUPI-G network and WRF-Chem simulations for three different emission scenarios in four regions of northwest India: North Punjab, Southwest Punjab, Central Haryana, and Delhi-NCR are shown from October 16 to November 30, 2022 (Fig. S10a), 2023 (Fig. 6) and 2023 (Fig. S10b). The modelled concentrations for all three scenarios generally track the pattern of observed concentrations, but with noticeable differences for all 3 years. The WRF-CTL scenario shows reasonable agreement with the observed data, particularly in North Punjab and South Punjab (Table 3), given the uncertainties in emissions (addressed in Section 3.5), chemical scheme and meteorology. For all four regions, the observed $PM_{2.5}$ concentrations tend to increase over the course of intense biomass burning days shown in Fig. 2, with the highest concentrations (200 μg m^{-3}) occurring by mid-November. The inter annual difference in WRF-CTL

concentration at a level of ≥200 μg m^{-3} over Southwest Punjab during the second week of November in 2023, because of difference in CRB activities among the year. The modelled concentrations fail to capture some of the episodes of high polluting days, for example November 9 in 2022 and November 2 in 2022 due to the absence of satellite-derived fire counts during hazy cloudy days (ref. Fig. S4 and S5).

The WRF-Chem model is underestimating $PM_{2.5}$ concentrations over Delhi-NCR in 2022 and most of the days of 2023. During the starting and ending days of CRB season the model is doing fairly well with the observed concentration showing the uncertainties and contribution share associated with the BB emission. The WRF-PUBB and WRF-CTL showed similar magnitude across all the days for all four regions in 2022 and 2023, however, in some days of November month for Punjab shows some minor differences. This indicates the dominant share of Punjab BB emissions to the overall concentration over the regions, which is clearly seen from the map plots during 3 different periods of 16–30 October, 1–15 November and 16–30 November 2022 (Fig. S3).

The CRB contribution in Fig. 6 (light green bars) is high (30–50%) in mid-October 2023, and then decreased over time, consistently with observed fire counts. This suggests that BB was a significant source of $PM_{2.5}$ in North Punjab early in the observation period, with its influence diminishing later. Compared to North Punjab, the CRB contribution is 40–70% in Southwest Punjab, which was the highest among all three
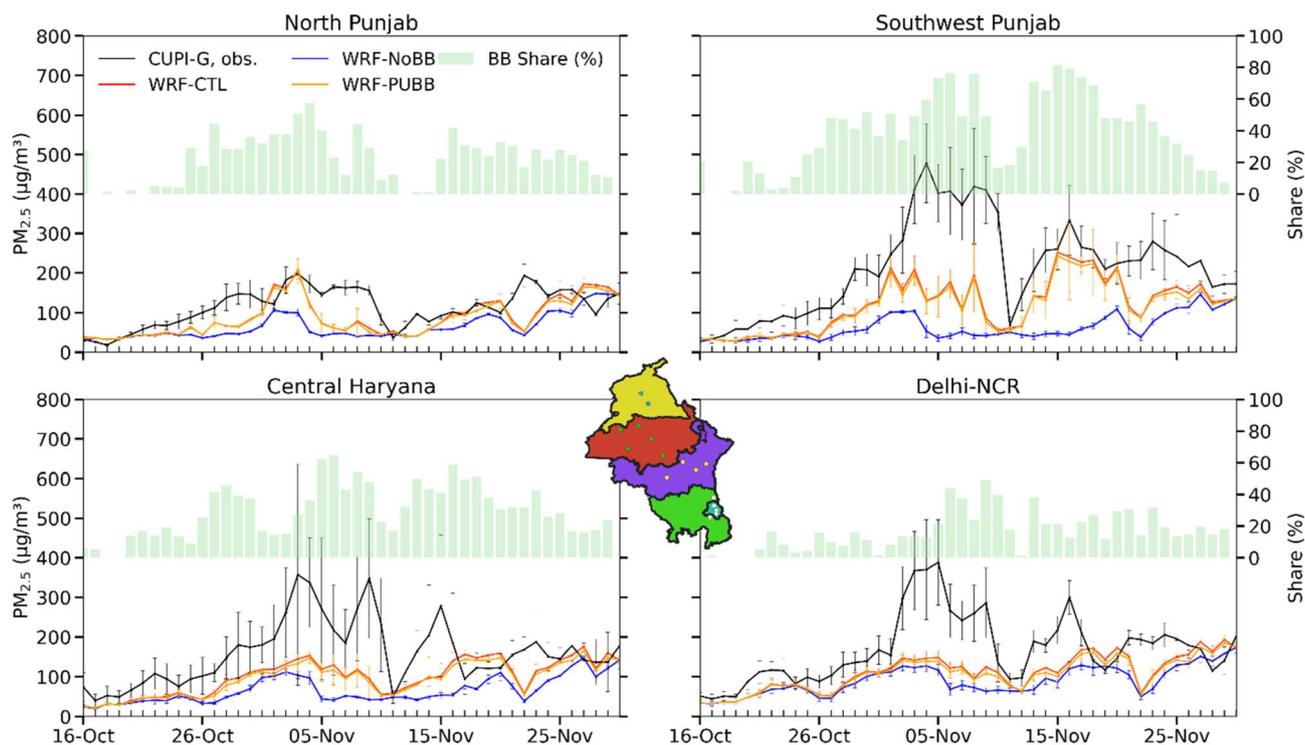

Fig. 6 Evolution of daily average concentration as observed by CUPI-Gs and the WRF-NoBB, WRF-PUBB and WRF-CTL simulations for 2023. The light-green bar shows the percentage share of $PM_{2.5}$ due to biomass burning emissions (eqn (1)). Four regions and the sites used in the regional averaging are shown schematically in the map at the center of 4 panels (see also Fig. 3 for better clarity). Results for 2022 and 2024 are shown in Fig. S10a and b, respectively.

1220 | *Environ. Sci.: Atmos.*, 2025, **5**, 1211–1229

© 2025 The Author(s). Published by the Royal Society of Chemistry

regions in November 2023. Among the four regions, Delhi-NCR had the least CRB contribution of around 20% in average, which increase further to 50% during specific days with direct plume from CRB hotspots. These specific events were limited to 2–3 days in most favorable downwind conditions and observed from CUPI-G observations.[18,19]

The average CRB shares to $PM_{2.5}$ in 2022 (Fig. S10a) are similar to those estimated for 2023 in all four regions, but due to the prolonged burning in the month of October and November the CRB share is frequently above 20% from the third week of October 2023 for all 4 regions. In 2024 the lower CRB share is observed in all regions, especially over Delhi (Fig. S10b), due to very low magnitude of CRB (FINN-NRT) emissions compared to 2023 and 2022 (Fig. 2). Possible reasons for underestimation of emissions by FINN-NRT are discussed later in Section 3.5.

3.4 CRB induced increment in $PM_{2.5}$ concentration

The bar chart (Fig. 7) shows the summary of CRB contribution to $PM_{2.5}$ concentrations in four regions of observation network from 16 October to 30 November 2022, 2023 and 2024. The estimated CRB contribution (mean ± 1-sigma standard deviation) over Delhi-NCR ranged 18 ± 14% in 2022, 16 ± 13% in 2023, and 9 ± 29% in 2024. Similarly, in Central Haryana, CRB accounted 25 ± 16% in 2022, 31 ± 17% in 2023, and 9 ± 49% in 2024, reflecting an increase in 2023 before sharply dropping in 2024. However, the estimated values of Southwest Punjab ranged 39 ± 22% in 2022, 48 ± 25% in 2023, and 27 ± 47% in 2024, making it the most impacted region by CRB emissions. In North Punjab, the CRB contribution ranged 28 ± 16% in 2022, 24 ± 16% in 2023, and 11 ± 41% in 2024. The prolonged CRB activities over Southwest Punjab in 2023 could not have much impact on the CRB induced $PM_{2.5}$ over Delhi due to the absence of direct plume from the source to Delhi-NCR (see Mangaraj

et al. for a discussion on the meteorological conditions).[19] For the year 2024 the BB contribution share is reduced by half across all regions due to very low BB emission days in 2024 (Fig. 2). It is very interesting that the BB contribution over the CRB source region of southwest Punjab also dropped significantly in the year 2024.

Our results are in overall agreement with previous studies, but the details differ as we can use large number of measurements from the CRB emission regions. Kulkarni et al.[12] found that CRB contributes approximately 20% to $PM_{2.5}$ levels, with a range of 50–70% on CRB dominated days, while Saharan et al.[23] found CRB contribution of 30–60% and highlighted dominant share of CRB emission by certain hotspot districts, similar to southwest Punjab region of this study. Govardhan et al.[15] reported 15% of mean contribution with a 35–40% range, based on the FINN inventory. Nagar and Sharma[50] also used FINN inventory and reported a contribution of 31 ± 16% during October to December of 2013 and 2014. Awasthi et al.[51] positive matrix factorization (PMF) analysis of 111 volatile organic compounds and $PM_{2.5}$ during 15th August to 26th November suggests contribution of CRB to $PM_{2.5}$ is 23%.

3.5 Additional scenarios to understand the uncertainties and future scopes

3.5.1 Missing emission days. Fig. 8 illustrates the simulation results for the years 2022 and 2023 after accounting for missing biomass burning emission days in the model (statistics in Table 4). The results cover the period from November 1 to 15 for both years, during which missing emissions were filled for days with cloud cover. However, it is important to note the potential limitation of this approach, as there might have been no biomass burning on certain days, such as on 11 November 2023, due to widespread rainfall, but emissions being included in the model.
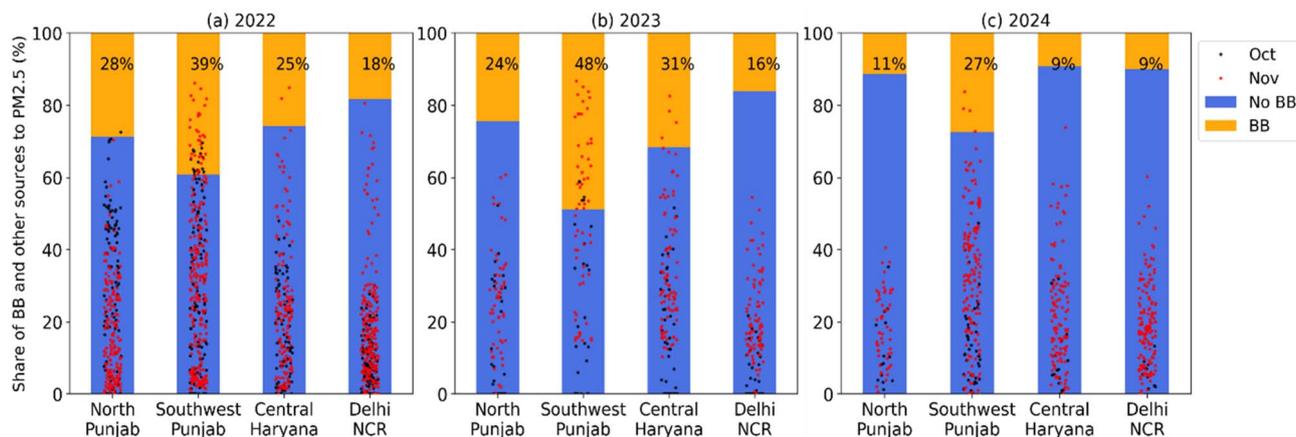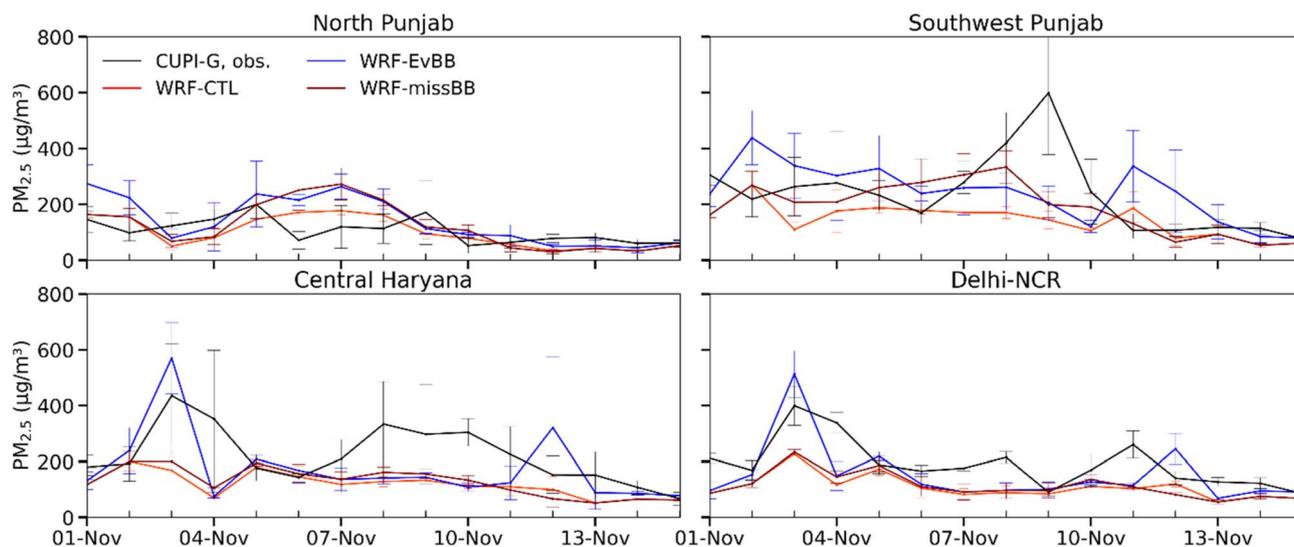

Fig. 7 Stack bar plot showing the average contribution share of biomass burning and other emission share for the October and November of 2022 (a), 2023 (b) and 2024 (c). The blue bars represent the share of other emissions and the stacked orange, show the biomass burning contribution from the WRF-Chem model. The black and red dots represent the daily contribution for October and November, respectively, in a strip-plot. The 2024 simulation uses the FINN-NRT BB emission as opposed to 2022 and 2023 based on FINN-v2.5 BB emissions. The horizontal jitter (i.e., the spread along the x-axis) for black and red dots within each bar does not represent a numeric x-value, but for better clarity in display of values by day within the month of Oct–Nov (https://seaborn.pydata.org/generated/seaborn.stripplot.html).

© 2025 The Author(s). Published by the Royal Society of Chemistry

Environ. Sci.: Atmos., 2025, 5, 1211–1229 | **1221**

Fig. 8 Daily mean PM$_{2.5}$ concentration from CUPI-G observations and compared with WRF-CTL, WRF-missBB and WRF-EvBB simulations for 2022. The WRF-EvBB and WRF-missBB cases have not ran for the year 2023 and 2024 respectively. Available results for 2023 and 2024 are shown in Fig. S11a and b.

Table 4 WRF-missBB and WRF-EvBB model characteristics compared to the WRF-CTL based on daily mean PM$_{2.5}$ concentrations (units: μg m^{-3}). Significant effect of EvBB emission case on the mean bias, compared to the CTL case is observed for 2022 and 2024, while the missBB emission does not affect the mean biases significantly with respect to the CTL case. On average the mean bias diminishes for the WRF-EvBB simulation case in 2022, but that for 2024 only shows lesser bias suggesting major underestimation of the emissions. The changes in PM$_{2.5}$ for WRF-EvBB and WRF-missBB cases, relative to WRF-CTL, are given within the parenthesis in columns 5 and 6, respectively

Year	Region	Observed PM$_{2.5}$ (μg m^{-3})	Mean bias (model – observed) [% increase compared to CTL]			Correlation coefficient (r)		
			WRF-CTL	WRF-EvBB	WRF-missBB	WRF-CTL	WRF-EvBB	WRF-missBB
2022	Central Haryana	223	−59	−36[a] [14]	−55 [2]	0.55	0.62	0.68
2022	Delhi-NCR	181	−53	−37[a] [12]	−51 [2]	0.73	0.74	0.77
2022	North Punjab	109	−15	16[a] [33]	−8 [7]	0.35	0.46	0.36
2022	Southwest Punjab	233	−45	12[a] [30]	−30 [8]	0.58	0.52	0.73[a]
2023	Central Haryana	226	−62	NA[b]	−57 [3]	0.52	NA	0.55
2023	Delhi-NCR	262	−60	NA	−58 [1]	0.57	NA	0.58
2023	North Punjab	128	−27	NA	−26 [1]	0.56	NA	0.54
2023	Southwest Punjab	316	−95	NA	−86 [4]	0.65	NA	0.73
2024	Central Haryana	269	−137	−109[a] [21]	NA	0.35	0.46[a]	NA
2024	Delhi-NCR	175	−81	−63[a] [19]	NA	0.07	0.12	NA
2024	North Punjab	296	−114	−89[a] [13]	NA	0.58	0.60	NA
2024	Southwest Punjab	456	−192	−135[a] [21]	NA	0.70	0.78[a]	NA

[a] Indicates significant difference from WRF-CTL case. [b] NA – simulation not available.

For 2022, the inclusion of the missing emission days resulted in improved concentration over Southwest Punjab with a mean bias shifted from −45 to −30 (Table 4), reflecting improved agreement of WRF-missBB with the observation, compared to WRF-CTL. In North Punjab, the mean bias improved from −15 (WR-CTL) to −8 (WRF-missBB), highlighting better agreement with observed values, however, there is a noticeable over-estimating by the model during 5 to 9 November 2022. For Central Haryana and Delhi-NCR, slight reductions in mean bias are also noted, though the changes were less pronounced. Correlation coefficients (r) also show improvements, particularly for Southwest Punjab, where the correlation increased

from 0.58 (WRF-CTL) to 0.73 (WRF-missBB). This suggests that the temporal patterns of PM$_{2.5}$ are better captured when missing biomass burning days are incorporated into the simulation (Table 4). For 2023, the evolution of WRF-missBB scenario was flat particularly over the Southwest Punjab and the pattern suggesting the dominant role of meteorology. The WRF-missBB also failed to capture the peak concentration days (1 to 3 November) over Delhi which clarifies the role of local emissions.

3.5.2 Late afternoon emissions in 2024. The fire detection from satellites has been at specific times of the satellite over-pass and thus any change in the CRB timing will affect the FDCs

1222 | Environ. Sci.: Atmos., 2025, **5**, 1211–1229

© 2025 The Author(s). Published by the Royal Society of Chemistry

between years. Here the continuous measurements by CUPI-Gs along with hypothetical model simulation cases can be utilized for inferring the ground situation. There are discussions that the farmers might have changed the time of burning of the crop residue, typically from noon to late afternoon to avoid surveillance by the administrative agencies (various media reports). In 2024, the fire detection counts and burnt area are decreased by 53% and 58%, respectively, compared to 2023. A large decrease in CRB is expected to have an equally large impact on the reaction of air pollution under similar meteorological conditions. However, our observations of $PM_{2.5}$ do not show much reduction in the Punjab region; in fact, in late November the concentrations are higher in 2024 compared to 2023 (Fig. 6 and S10b). Such observations raise doubt in our mind if the farmers really have changed their practice of crop residue burning. To explain the high $PM_{2.5}$ concentrations under much lower emissions due to lower fire counts in 2024, we have made hypothetical changes to the diurnal profile of biomass burning emissions in our model (WRF-EvBB). Fig. 9 shows the distributions of $PM_{2.5}$ in the two simulation cases at 1:30 am local time. An animation of hourly mean $PM_{2.5}$ suggests that the high

CRB emission signal in the evening accumulates through the night and the surface concentrations remains higher on next day in the WRF-EvBB case compared to the WRF-CTL case (Animation 2).

In the WRF-EvBB scenario, the diurnal emission peak is shifted by four hours later into the afternoon at 6:30 pm local time compared to the WRF-CTL case at 2:30 pm (Fig. S6), aligning with the information from the local authorities and newspaper reports. This adjustment allows us to check a better representation of the real-world emission timings, particularly in regions with delayed burning practices. Fig. 10 shows the diurnal variation of $PM_{2.5}$ concentration from CUPI-G observation, WRF-CTL and WRF-EvBB over the northwest Indian states and Chandigarh. In general, we find that the WRF-CTL simulation for all three years underestimates the diurnal amplitude in the concentrations of $PM_{2.5}$ in all the regions (Fig. 10a, b and d–g). This is presumably because the model simulations underestimate the nighttime planetary boundary layer,[29] and thus the model simulates lower concentrations in the night by large amount compared to the observations. In contrast the mid-day concentrations are in better agreement between the
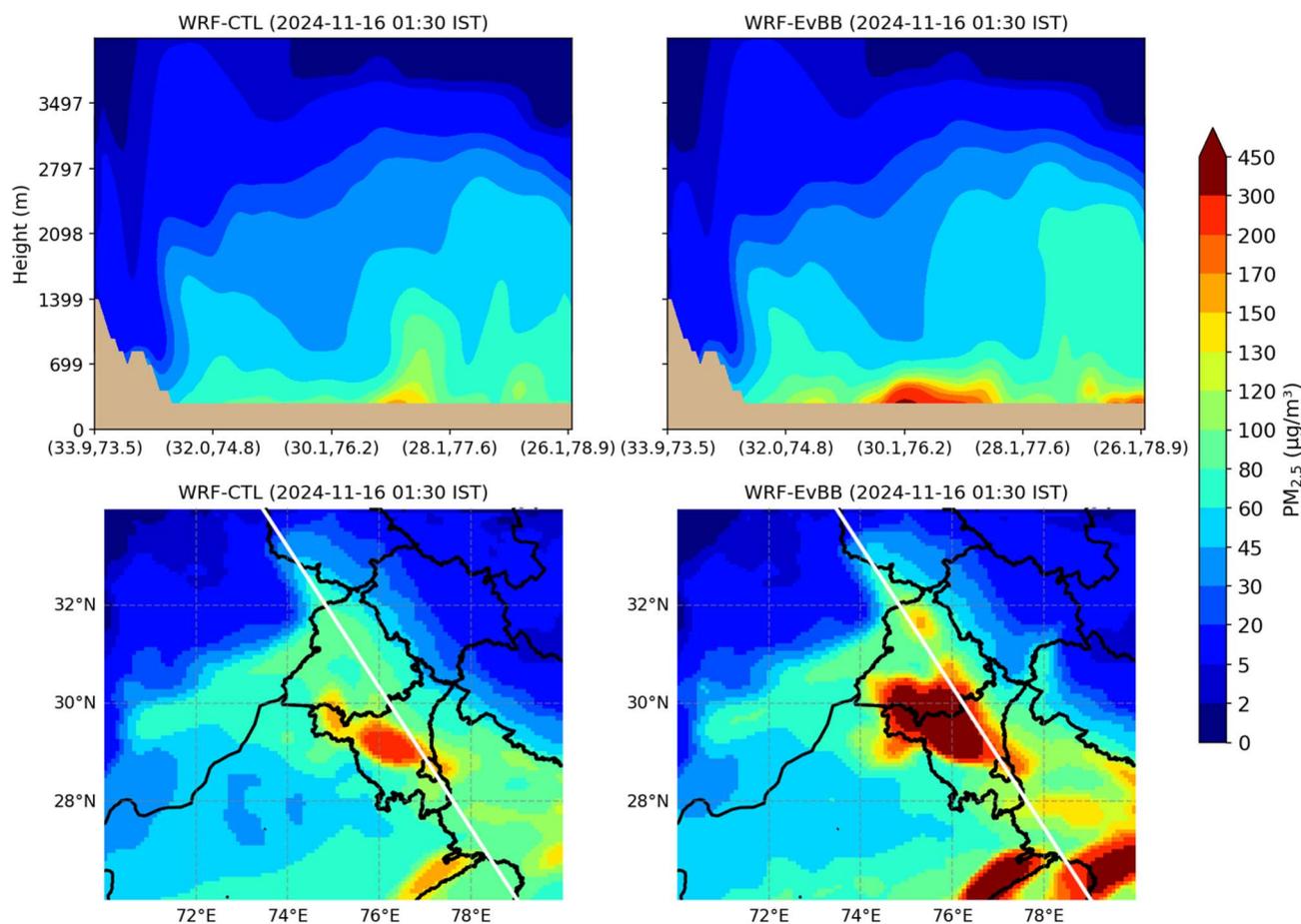
Fig. 9 Horizontal maps at model level 1 (bottom row) and vertical cross-sections (top row) of $PM_{2.5}$ concentration on 16 November 2024, 1:30 local time (IST) over domain 2 of the model for the cases WRF-CTL (left column) and WRF-EvBB (right column). The thin white line crossing over the horizontal maps, starting at 33.9°N, 73.5°E and ending at 26.1°N, 78.9°E, shows the line of cross-section selected for the vertical distributions. Animation 2 shows the evolution of $PM_{2.5}$ in the region during 1–16 November 2024, as given in the supplement. The choice of cross-section positioning is made to show the mechanism of transport of CRB emission signals from Punjab to Delhi and beyond. In particular, the uplifting of CRB emissions from the boundary layer to the free troposphere and its diurnal variabilities are seen from the animation.
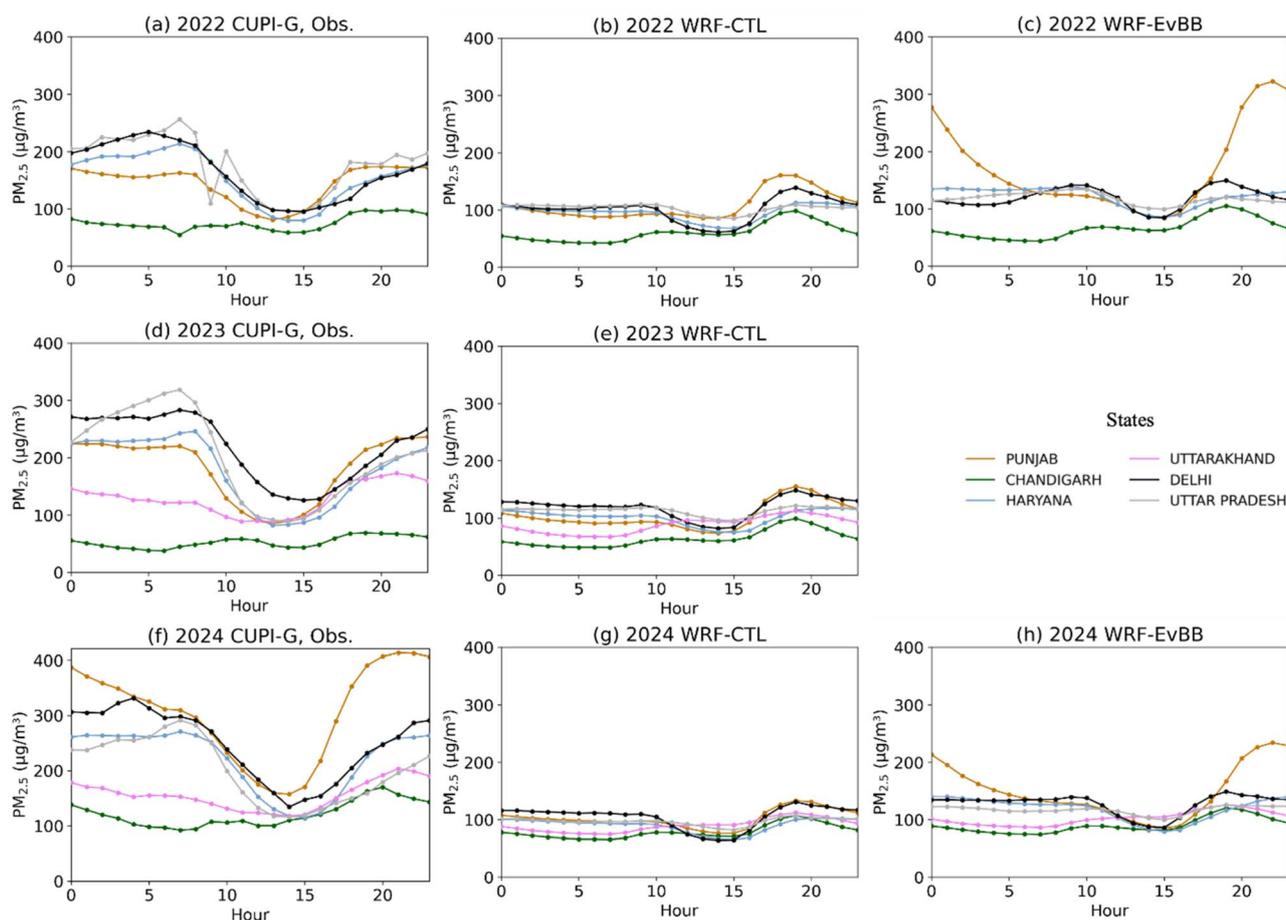
© 2025 The Author(s). Published by the Royal Society of Chemistry

Environ. Sci.: Atmos., 2025, **5**, 1211–1229 | **1223**

Fig. 10 Diurnal PM$_{2.5}$ concentration for all three years from CUPI-G observation (left column; (a, d and f)) and WRF–Chem model simulation with two scenarios of WRF-CTL (middle column; (b, e and g)) and WRF-EvBB (right column; (c and h); results for 2023 missing). Results are shown as the mean of 1–15 November of 2022 (top row; (a–c)), 2023 (middle row; (d and e)) and 2024 (bottom row; (f–h)). The 2024 simulation uses the BB emissions from FINN-NRT, while 2022 and 2023 simulations used FINN-v2.5.

model and observations. The nighttime bias in WRF-CTL simulations can also be partly responsible for the overall underestimation of daily-mean PM$_{2.5}$ as seen in Fig. 6 and S10a, b.

For 2024, WRF-EvBB shows improved performance by capturing the evening concentration peaks more effectively over Punjab, Delhi and Haryana compared to the WRF-CTL scenario. The mean bias in WRF-EvBB has been reduced across all the stations which confirms the homogenous impact of the late afternoon burning emissions. Over Punjab, even with lower emissions in 2024 compared to 2022, the WRF-EvBB scenario successfully achieves similar evening time PM$_{2.5}$ concentration levels. This indicates that the newly adjusted timing of emissions in WRF-EvBB aligns well with the theory of late afternoon burning practices, which is likely to have been practiced well before 2024. Thus, a better representation of diurnal profile of emissions is critical for improved simulations of air pollutants and the chemical constituents in general in the atmosphere. A smaller amount of emissions in the evening has greater impact on the daily mean concentrations because the planetary boundary layer height is low in the evening and persists throughout the night (Fig. 10b, c, g and h).

This finding has large implications when the atmospheric chemistry-transport models are used for validation of the emission inventories, without incorporating an accurate diurnal profile. As mentioned in the methods section, the chemical scheme GOCART in WRF-Chem does not include secondary organic aerosol (SOA) formation. This could be one of the main reasons for gross underestimation of the observed PM$_{2.5}$ for the WRF-CTL case (Table 4). However, the sensitivity simulations suggest that the WRF-missBB or WRF-EvBB cases overestimated PM$_{2.5}$ in the two Punjab regions, but continues to underestimate for Central Haryana and Delhi-NCR in 2022. Whether the lack of SOA formation due to CRB emissions is main cause of this underestimation in the downwind regions of Punjab or that due to missing Delhi-NCR's industrial emissions[38] cannot be judged from the existing measurements.[52] While the CUPI-G measurement network provides only basic air pollutant data, the advanced measurement systems are established only in the city areas[52] and cannot distinguish between local *vs.* outside the domain contribution to urban air pollutants. The large underestimations of the observed PM$_{2.5}$ by all 3 model cases and all regions in 2023 and 2024 point toward significant underestimation of emissions (Table 4). Any role of

1224 | *Environ. Sci.: Atmos.*, 2025, **5**, 1211–1229

© 2025 The Author(s). Published by the Royal Society of Chemistry

SOA formation from CRB emissions would increase the share of biomass burning contributions to $PM_{2.5}$ in Central Haryana and Delhi-NCR compared to those given in Fig. 7.

A shift in residue burning time to evening, in opposed to conventional early afternoon burning time, has far reaching manifestation in terms of policy implementation. As seen from the map plots in Fig. 5 and S9 that the high $PM_{2.5}$ plumes from Punjab CRB goes far beyond in the case of WRF-EvBB, compared to the case of WRF-CTL. This implies the effect of emissions in the evening has a much greater impact on the $PM_{2.5}$ levels on the surface, compared to when the same amount of emissions occur mid-day. If the farmers are burning crop residues in the afternoon just to avoid surveillance by the remote sensing satellites, we must avoid such a situation by educating them. And this is possible by developing an understanding between the farmers and policymakers regarding how soon we would like to achieve the targeted zero CRB. Further analysis is needed to clearly identify the role of secondary aerosol production in the night when the humidity is high, compared to the day, and how the trapping of pollutants in the shallow boundary layer differs in mixing vertically and spread horizontally in that atmosphere.

4 Conclusions

WRF-Chem is used under five distinct CRB emission scenarios to study the impact of these emission on $PM_{2.5}$ concentration over northwestern India. The simulated concentration is compared with the CUPI-G measurements, where the model underestimates the observed high magnitude of $PM_{2.5}$ concentration, however, it efficiently produced temporal evolution of $PM_{2.5}$ during the intense CRB days. Following are the major conclusions of this study:

(1) CRB emission derived from satellite observations shows a progressive decreasing trend over Punjab and Haryana (2022–2024), due to which, the mean contribution of CRB to Delhi $PM_{2.5}$ was reduced dramatically from 18% and 16% in 2022 and 2023, respectively, to 9% in 2024, with a very high range of day-to-day variability. However, the observed $PM_{2.5}$ from CUPI-G sensor network shows continuously high $PM_{2.5}$ over the rural sites of Punjab, evidently highlighting the limitation of the current modelling systems.

(2) WRF-missBB and WRF-EvBB scenario are designed to understand the possible limitation of existing CRB emission input for models. These scenarios improved the simulation and captured the observed spatial and temporal variation of $PM_{2.5}$, relative to the control simulation. Incorporating missing CRB emission days substantially enhances model performance by reducing model-observed biases and better capturing observed temporal dynamics, particularly in regions heavily influenced by burning events.

(3) The diurnal cycle of $PM_{2.5}$ in 2024 shows an unusual early evening concentration over Punjab, which suggests a shift in CRB activities adopted by the farmers, possibly to escape from satellite detection.[53] Considering the adverse effects of high pollution levels caused by evening CRB emissions, farmers should be consulted through awareness programs. The diurnal

profile of CRB emission must be carefully accounted in the global/regional emission inventories by improving FDC and BA detection from geostationary or a constellation of polar orbiting satellite sensors.

5 Additional information

Aakash CUPI-G team list

Sanjeev Bhardwaj (Department of Environment Studies, Panjab University, Chandigarh, India), Manpreet S. Bhatti (Department of Botanical and Environmental Sciences, Guru Nanak Dev University, Amritsar, Punjab, India), Surendra K. Dhaka (Radio and Atmospheric Physics Lab, Rajdhani College, University of Delhi, New Delhi, India), A. P. Dimri (School of Environmental Sciences, Jawaharlal Nehru University, New Delhi, India), Dilip Ganguly (Centre for Atmospheric Sciences, Indian Institute of Technology Delhi, New Delhi, India), Sachiko Hayashida (Research Institute for Humanity and Nature, Kyoto, Japan), Mizuo Kajino (Meteorological Research Institute, Japan Meteorological Agency, Ibaraki, Japan), Ravi K. Kunchala (Centre for Atmospheric Sciences, Indian Institute of Technology Delhi, New Delhi, India), Shristy Malik (Department of Applied Physics, Delhi Technological University, Delhi, India), Tuhin K. Mandal (Environmental Sciences & Biomedical Metrology Division, CSIR-National Physical Laboratory, New Delhi, India), Prakhar Misra (Dept. of Civil Engineering, Indian Institute of Technology Roorkee, Uttarakhand, India), Sahil Mor (Department of Environmental Science Engineering, Guru Jambheshwar University of Science and Technology, Hisar, India), Suman Mor (Department of Environment Studies, Panjab University, Chandigarh, India), Manish K. Naja (Aryabhatta Research Institute of Observational Sciences, Manora Peak, Nainital, Uttarakhand, India), Khaiwal Ravindra (Department of Community Medicine and School of Public Health, Postgraduate Institute of Medical Education and Research, Chandigarh, India), Aka Sharma (School of Environmental Sciences, Jawaharlal Nehru University, New Delhi, India), Tanbir Singh (SCVB Government College, Palampur, Himachal Pradesh, India), Kamal Vatta (Department of Economics and Sociology, Punjab Agricultural University, Ludhiana, Punjab, India), Kazuyo Yamaji (Graduate School of Maritime Sciences, Kobe University, Kobe, Japan).

Author contributions

AB and PKP designed WRF-Chem simulation experiments, finalised the analysis and led preparation of the manuscript draft; MT, JSHB helped with model initial set up on ES4 at JAMSTEC and provided useful discussion on data analysis; PM performed gridded analysis from site data and provided useful input for preparation of first draft; YM, TN assembled, calibrated and deployed CUPI-G sensors; NY, HA helped data management and various analysis; VS provided perspectives on air pollution in Delhi-NCR and provided useful discussion on results; all coauthor contributed to preparation of the text and approved the manuscript. The Aakash CUPI-G team helped

© 2025 The Author(s). Published by the Royal Society of Chemistry

Environ. Sci.: Atmos., 2025, 5, 1211–1229 | 1225

maintenance of observational network in the northwestern India region.

Conflicts of interest

Authors declare no competing interests.

Data availability

All measured $PM_{2.5}$ data at hourly time average are available at RIHN Aakash website, https://aakash-rihn.org/en/data-set/. Some of the spatial map analysis of daily $PM_{2.5}$ variabilities along with meteorological conditions are available at https://zenodo.org/records/15702750. Model simulations are available from our data archival (on request to the authors).

Supplementary information is available. See DOI: https://doi.org/10.1039/d5ea00052a.

Acknowledgements

References

1 *WHO ambient air quality database, 2022 update: status report*, World Health Organization, Geneva, 2023.

2 Institute for Health Metrics and Evaluation, *Global Burden of Disease Study 2021 (GBD 2021) Air Pollution Exposure Estimates 1990–2021*, 2024, DOI: 10.6069/VKDR-QY60.

3 R. Sawlani, R. Agnihotri, C. Sharma, P. K. Patra, A. P. Dimri, K. Ram and R. L. Verma, The Severe Delhi SMOG of 2016: A Case of Delayed Crop Residue Burning, Coincident Firecracker Emissions, and Atypical Meteorology, *Atmos. Pollut. Res.*, 2019, **10**(3), 868–879, DOI: 10.1016/j.apr.2018.12.015.

4 V. Singh, S. Singh and A. Biswal, Exceedances and Trends of Particulate Matter (PM2.5) in Five Indian Megacities, *Sci. Total Environ.*, 2021, **750**, 141461, DOI: 10.1016/j.scitotenv.2020.141461.

5 Chetna, S. K. Dhaka, S.-E. Walker, V. Rawat and N. Singh, Decoding Temporal Patterns and Trends of PM10 Pollution over Delhi: A Multi-Year Analysis (2015–2022), *Environ. Monit. Assess.*, 2024, **196**(6), 500, DOI: 10.1007/s10661-024-12638-7.

6 A. Roychowdhury and S. Kaur, *Delhi at risk of losing its long term air quality gains*, 2024, https://www.cseindia.org/2024-delhi-at-risk-of-losing-its-long-term-air-quality-gains-12563, accessed 2025-04-27.

7 P. Misra, M. Takigawa, P. Khatri, S. K. Dhaka, A. P. Dimri, K. Yamaji, M. Kajino, W. Takeuchi, R. Imasu, K. Nitta, P. K. Patra and S. Hayashida, Nitrogen Oxides Concentration and Emission Change Detection during COVID-19 Restrictions in North India, *Sci. Rep.*, 2021, **11**(1), 9800, DOI: 10.1038/s41598-021-87673-2.

8 V. Kumar, S. Giannoukos, S. L. Haslett, Y. Tong, A. Singh, A. Bertrand, C. P. Lee, D. S. Wang, D. Bhattu, G. Stefenelli, J. S. Dave, J. V. Puthussery, L. Qi, P. Vats, P. Rai, R. Casotto, R. Satish, S. Mishra, V. Pospisilova, C. Mohr, D. M. Bell, D. Ganguly, V. Verma, N. Rastogi, U. Baltensperger, S. N. Tripathi, A. S. H. Prévôt and J. G. Slowik, Highly Time-Resolved Chemical Speciation and Source Apportionment of Organic Aerosol Components in Delhi, India, Using Extractive Electrospray Ionization Mass Spectrometry, *Atmos. Chem. Phys.*, 2022, **22**(11), 7739–7761, DOI: 10.5194/acp-22-7739-2022.

9 N. Nirwan, A. Siddiqui, H. b. s. Kannemadugu, P. Chauhan and R. P. Singh, Determining Hotspots of Gaseous Criteria Air Pollutants in Delhi Airshed and Its Association with Stubble Burning, *Sci. Rep.*, 2024, **14**(1), 986, DOI: 10.1038/s41598-023-51140-x.

10 S. N. Tripathi, S. Yadav and K. Sharma, Air Pollution from Biomass Burning in India, *Environ. Res. Lett.*, 2024, **19**(7), 073007, DOI: 10.1088/1748-9326/ad4a90.

11 C. Venkataraman, A. Anand, S. Maji, N. Barman, D. Tiwari, K. Muduchuru, A. Sharma, G. Gupta, A. Bhardwaj, D. Haswani, D. Pullokaran, K. Yadav, R. Sunder Raman, M. Imran, G. Habib, T. S. Kapoor, G. Anurag, R. Sharma, H. C. Phuleria, A. M. Qadri, G. K. Singh, T. Gupta, A. Dhandapani, R. N. Kumar, S. Mukherjee, A. Chatterjee, S. Rabha, B. K. Saikia, P. Saikia, D. Ganguly, P. Chaudhary, B. Sinha, S. Roy, A. Muthalagu, A. Qureshi, Y. Lian, G. Pandithurai, L. Prasad, S. Murthy, S. S. Duhan, J. S. Laura, A. K. Chhangani, T. A. Najar, A. Jehangir, A. P. Kesarkar and V. Singh, Drivers of PM2.5 Episodes and Exceedance in India: A Synthesis From the COALESCE Network, *J. Geophys. Res.:Atmos.*, 2024, **129**(14), e2024JD040834, DOI: 10.1029/2024JD040834.

12 S. H. Kulkarni, S. D. Ghude, C. Jena, R. K. Karumuri, B. Sinha, V. Sinha, R. Kumar, V. K. Soni and M. Khare, How Much Does Large-Scale Crop Residue Burning Affect the Air Quality in Delhi?, *Environ. Sci. Technol.*, 2020, **54**(8), 4790–4799, DOI: 10.1021/acs.est.0c00329.

13 G. Beig, S. K. Sahu, V. Singh, S. Tikle, S. B. Sobhana, P. Gargeva, K. Ramakrishna, A. Rathod and B. S. Murthy, Objective Evaluation of Stubble Emission of North India and Quantifying Its Impact on Air Quality of Delhi, *Sci. Total Environ.*, 2020, **709**, 136126, DOI: 10.1016/j.scitotenv.2019.136126.

14 H. Sembhi, M. Wooster, T. Zhang, S. Sharma, N. Singh, S. Agarwal, H. Boesch, S. Gupta, A. Misra, S. N. Tripathi, S. Mor and R. Khaiwal, Post-Monsoon Air Quality Degradation across Northern India: Assessing the Impact of Policy-Related Shifts in Timing and Amount of Crop

Residue Burnt, *Environ. Res. Lett.*, 2020, **15**(10), 104067, DOI: 10.1088/1748-9326/aba714.

15 G. Govardhan, R. Ambulkar, S. Kulkarni, A. Vishnoi, P. Yadav, B. A. Choudhury, M. Khare and S. D. Ghude, Stubble-Burning Activities in North-Western India in 2021: Contribution to Air Pollution in Delhi, *Heliyon*, 2023, **9**(6), e16939, DOI: 10.1016/j.heliyon.2023.e16939.

16 T. Mukherjee, V. Vinoj, S. K. Midya, S. P. Puppala and B. Adhikary, Numerical Simulations of Different Sectoral Contributions to Post Monsoon Pollution over Delhi, *Heliyon*, 2020, **6**(3), e03548, DOI: 10.1016/j.heliyon.2020.e03548.

17 J. S. H. Bisht, P. K. Thapliyal, M. V. Shukla and R. Kumar, A Comparative Study of Different AIRS Products for the Detection of Near-Surface Temperature Inversion: A Case Study over New Delhi, *Remote Sensing Letters*, 2013, **4**(1), 94–103, DOI: 10.1080/2150704X.2012.698321.

18 T. Singh, Y. Matsumi, T. Nakayama, S. Hayashida, P. K. Patra, N. Yasutomi, M. Kajino, K. Yamaji, P. Khatri, M. Takigawa, H. Araki, Y. Kurogi, M. Kuji, K. Muramatsu, R. Imasu, A. Ananda, A. A. Arbain, K. Ravindra, S. Bhardwaj, S. Kumar, S. Mor, S. K. Dhaka, A. P. Dimri, A. Sharma, N. Singh, M. S. Bhatti, R. Yadav, K. Vatta and S. Mor, Very High Particulate Pollution over Northwest India Captured by a High-Density in Situ Sensor Network, *Sci. Rep.*, 2023, **13**(1), 13201, DOI: 10.1038/s41598-023-39471-1.

19 P. Mangaraj, Y. Matsumi, T. Nakayama, A. Biswal, K. Yamaji, H. Araki, N. Yasutomi, M. Takigawa, P. K. Patra, S. Hayashida, A. Sharma, A. P. Dimri, S. K. Dhaka, M. S. Bhatti, M. Kajino, S. Mor, R. Khaiwal, S. Bhardwaj, V. J. Vazhathara, R. K. Kunchala, T. K. Mandal, P. Misra, T. Singh, K. Vatta and S. Mor, Weak Coupling of Observed Surface PM2.5 in Delhi-NCR with Rice Crop Residue Burning in Punjab and Haryana, *npj Clim. Atmos. Sci.*, 2025, **8**(1), 1–9, DOI: 10.1038/s41612-025-00901-8.

20 Balwinder-Singh, A. J. McDonald, A. K. Srivastava and B. Gerard, Addendum: Tradeoffs between Groundwater Conservation and Air Pollution from Agricultural Fires in Northwest India, *Nat. Sustain.*, 2020, **3**(11), 972, DOI: 10.1038/s41893-020-00632-z.

21 M. Agarwala, S. Bhattacharjee and A. Dasgupta, Unintended Consequences of Indian Groundwater Preservation Law on Crop Residue Burning, *Econ. Lett.*, 2022, **214**, 110446, DOI: 10.1016/j.econlet.2022.110446.

22 R. Lan, S. D. Eastham, T. Liu, L. K. Norford and S. R. H. Barrett, Air Quality Impacts of Crop Residue Burning in India and Mitigation Alternatives, *Nat. Commun.*, 2022, **13**(1), 6537, DOI: 10.1038/s41467-022-34093-z.

23 U. S. Saharan, R. Kumar, S. Singh, T. K. Mandal, M. Sateesh, S. Verma and A. Srivastava, Hotspot Driven Air Pollution during Crop Residue Burning Season in the Indo-Gangetic Plain, India, *Environ. Pollut.*, 2024, **350**, 124013, DOI: 10.1016/j.envpol.2024.124013.

24 A. Patel, R. Satish and N. Rastogi, Remarkably High Oxidative Potential of Atmospheric PM2.5 Coming from a Large-Scale Paddy-Residue Burning over the Northwestern Indo-Gangetic Plain, *ACS Earth Space Chem.*, 2021, **5**(9), 2442–2452, DOI: 10.1021/acsearthspacechem.1c00125.

25 A. Mhawish, C. Sarangi, P. Babu, M. Kumar, M. Bilal and Z. Qiu, Observational Evidence of Elevated Smoke Layers during Crop Residue Burning Season over Delhi: Potential Implications on Associated Heterogeneous PM2.5 Enhancements, *Rem. Sens. Environ.*, 2022, **280**, 113167, DOI: 10.1016/j.rse.2022.113167.

26 P. Goyal, S. Gulia and S. K. Goyal, Critical Review of Air Pollution Contribution in Delhi Due to Paddy Stubble Burning in North Indian States, *Atmos. Environ.*, 2025, **346**, 121058, DOI: 10.1016/j.atmosenv.2025.121058.

27 M. Kajino, K. Ishijima, J. Ching, K. Yamaji, R. Ishikawa, T. Kajikawa, T. Singh, T. Nakayama, Y. Matsumi, K. Kojima, T. Machida, T. Maka, P. K. Patra and S. Hayashida, Impact of Post Monsoon Crop Residue Burning on $PM_{2.5}$ over North India: Optimizing Emissions Using a High-Density in Situ Surface Observation Network, *Atmos. Chem. Phys.*, 2025, **25**, 7137–7160, DOI: 10.5194/acp-25-7137-2025.

28 P. K. Patra, N. Yasutomi, H. Araki, A. Biswal, P. Mangaraj, S. Hayashida, H. Asada, M. S. Bhatti, S. K. Das, S. K. Dhaka, A. P. Dimri, D. Ganguly, R. Imasu, K. Inubushi, P. Joshi, M. Kajino, P. Khatri, D.-G. Kim, R. K. Kunchala, T. K. Mandal, Y. Matsumi, C. M. Mehta, P. Misra, S. Mor, K. Muramatsu, R. Murao, M. K. Naja, T. Nakayama, E. Nishihara, K. Onishi, K. Ravindra, T. Sato, T. Singh, S. Sudo, K. Sugihara, M. Takigawa, K. Ueda, T. Umemura, K. Vatta and K. Yamaji, *Aakash Project: Towards mitigating particulate air pollution for improved public health along with sustainable agriculture in Northwest India*, Summary of research outcomes for stakeholder during 2020-2025, 2025, pp. 1–52, ISBN 978-4- 910834-48-1(online and print).

29 J. Rathore, D. Ganguly, V. Singh, M. Gupta, V. J. Vazhathara, A. Biswal, R. K. Kunchala, P. K. Patra, L. K. Sahu, S. Gani and S. Dey, Characteristics of Haze Pollution Events During Biomass Burning Period at an Upwind Site of Delhi, *J. Geophys. Res.:Atmos.*, 2025, **130**(7), e2024JD042347, DOI: 10.1029/2024JD042347.

30 C. Wiedinmyer, S. K. Akagi, R. J. Yokelson, L. K. Emmons, J. A. Al-Saadi, J. J. Orlando and A. J. Soja, The Fire INventory from NCAR (FINN): A High Resolution Global Model to Estimate the Emissions from Open Burning, *Geosci. Model Dev.*, 2011, **4**(3), 625–641, DOI: 10.5194/gmd-4-625-2011.

31 C. Wiedinmyer, Y. Kimura, E. C. McDonald-Buller, L. K. Emmons, R. R. Buchholz, W. Tang, K. Seto, M. B. Joseph, K. C. Barsanti, A. G. Carlton and R. Yokelson, The Fire Inventory from NCAR Version 2.5: An Updated Global Fire Emissions Model for Climate and Chemistry Applications, *Geosci. Model Dev.*, 2023, **16**(13), 3873–3891, DOI: 10.5194/gmd-16-3873-2023.

32 S. K. Akagi, R. J. Yokelson, C. Wiedinmyer, M. J. Alvarado, J. S. Reid, T. Karl, J. D. Crounse and P. O. Wennberg,

© 2025 The Author(s). Published by the Royal Society of Chemistry

Environ. Sci.: Atmos., 2025, **5**, 1211–1229 | **1227**

Emission Factors for Open and Domestic Biomass Burning for Use in Atmospheric Models, *Atmos. Chem. Phys.*, 2011, **11**(9), 4039–4072, DOI: **10.5194/acp-11-4039-2011**.

33 S. Binte Shahid, F. G. Lacey, C. Wiedinmyer, R. J. Yokelson and K. C. Barsanti, NEIVAv1.0: Next-Generation Emissions InVentory Expansion of Akagi et al. (2011) Version 1.0, *Geosci. Model Dev.*, 2024, **17**(21), 7679–7711, DOI: **10.5194/gmd-17-7679-2024**.

34 W. Hua, S. Lou, X. Huang, L. Xue, K. Ding, Z. Wang and A. Ding, Diagnosing Uncertainties in Global Biomass Burning Emission Inventories and Their Impact on Modeled Air Pollutants, *Atmos. Chem. Phys.*, 2024, **24**(11), 6787–6807, DOI: **10.5194/acp-24-6787-2024**.

35 T. Liu, L. J. Mickley, S. Singh, M. Jain, R. S. DeFries and M. E. Marlier, Crop Residue Burning Practices across North India Inferred from Household Survey Data: Bridging Gaps in Satellite Observations, *Atmos. Environ.:X*, 2020, **8**, 100091, DOI: **10.1016/j.aeaoa.2020.100091**.

36 H. Hersbach, B. Bell, P. Berrisford, S. Hirahara, A. Horányi, J. Muñoz-Sabater, J. Nicolas, C. Peubey, R. Radu, D. Schepers, A. Simmons, C. Soci, S. Abdalla, X. Abellan, G. Balsamo, P. Bechtold, G. Biavati, J. Bidlot, M. Bonavita, G. D. Chiara, P. Dahlgren, D. Dee, M. Diamantakis, R. Dragani, J. Flemming, R. Forbes, M. Fuentes, A. Geer, L. Haimberger, S. Healy, R. J. Hogan, E. Hólm, M. Janisková, S. Keeley, P. Laloyaux, P. Lopez, C. Lupu, G. Radnoti, P. d. Rosnay, I. Rozum, F. Vamborg, S. Villaume and J.-N. Thépaut, *Q. J. R. Meteorol. Soc.*, 2020, **146**, 1999–2049, DOI: **10.1002/qj.3803**.

37 P. Agarwal, D. S. Stevenson and M. R. Heal, Evaluation of WRF-Chem-Simulated Meteorology and Aerosols over Northern India during the Severe Pollution Episode of 2016, *Atmos. Chem. Phys.*, 2024, **24**(4), 2239–2266, DOI: **10.5194/acp-24-2239-2024**.

38 S. D. Ghude, G. Govardhan, R. Kumar, P. P. Yadav, R. Jat, S. Debnath, G. Kalita, C. Jena, S. Ingle, P. Gunwani, P. V. Pawar, R. Ambulkar, S. Kumar, S. Kulkarni, A. Kulkarni, M. Khare, A. Kaginalkar, V. K. Soni, N. Nigam, K. Ray, S. D. Atri, R. Nanjundiah and M. Rajeevan, Air Quality Warning and Integrated Decision Support System for Emissions (AIRWISE): Enhancing Air Quality Management in Megacities, *Bull. Am. Meteorol. Soc.*, 2024, E2525–E2550, DOI: **10.1175/BAMS-D-23-0181.1**.

39 K. Yamaji, S. Tsuji, M. Kajino, S. Hayashida, N. Yasutomi, H. Araki, A. Biswal, P. Mangaraj, Y. Matsumi, T. Nakayama, M. Takigawa, T. Singh and P. K. Patra, Modeling Study for the Heavy PM2.5 Pollution during the Dry Season in Northwestern India, *iCACGP/IGAC Conference*, Kuala Lumpur, 2024.

40 H. H. Shin and S.-Y. Hong, Representation of the Subgrid-Scale Turbulent Transport in Convective Boundary Layers at Gray-Zone Resolutions, *Mon. Weather Rev.*, 2015, **143**, 250–271, DOI: **10.1175/MWR-D-14-00116.1**.

41 J. Singh, N. Singh, N. Ojha, A. P. Dimri and R. S. Singh, Impacts of Different Boundary Layer Parameterization Schemes on Simulation of Meteorology over Himalaya, *Atmos. Res.*, 2024, **298**, 107154, DOI: **10.1016/j.atmosres.2023.107154**.

42 A. B. Guenther, X. Jiang, C. L. Heald, T. Sakulyanontvittaya, T. Duhl, L. K. Emmons and X. Wang, The Model of Emissions of Gases and Aerosols from Nature Version 2.1 (MEGAN2.1): An Extended and Updated Framework for Modeling Biogenic Emissions, *Geosci. Model Dev.*, 2012, **5**(6), 1471–1492, DOI: **10.5194/gmd-5-1471-2012**.

43 G. Janssens-Maenhout, M. Crippa, D. Guizzardi, F. Dentener, M. Muntean, G. Pouliot, T. Keating, Q. Zhang, J. Kurokawa, R. Wankmüller, H. Denier van der Gon, J. J. P. Kuenen, Z. Klimont, G. Frost, S. Darras, B. Koffi and M. Li, HTAP_v2.2: A Mosaic of Regional and Global Emission Grid Maps for 2008 and 2010 to Study Hemispheric Transport of Air Pollution, *Atmos. Chem. Phys.*, 2015, **15**(19), 11411–11432, DOI: **10.5194/acp-15-11411-2015**.

44 M. Crippa, D. Guizzardi, M. Muntean, E. Schaaf, F. Dentener, J. A. van Aardenne, S. Monni, U. Doering, J. G. J. Olivier, V. Pagliari and G. Janssens-Maenhout, Gridded Emissions of Air Pollutants for the Period 1970–2012 within EDGAR v4.3.2, *Earth Syst. Sci. Data*, 2018, **10**(4), 1987–2013, DOI: **10.5194/essd-10-1987-2018**.

45 T. Nakayama, Y. Matsumi, K. Kawahito and Y. Watabe, Development and Evaluation of a Palm-Sized Optical PM2.5 Sensor, *Aerosol Sci. Technol.*, 2018, **52**, 2–12, DOI: **10.1080/02786826.2017.1375078**.

46 P. Kumar, M. Khare, R. M. Harrison, W. J. Bloss, A. C. Lewis, H. Coe and L. Morawska, New Directions: Air Pollution Challenges for Developing Megacities like Delhi, *Atmos. Environ.*, 2015, **122**, 657–661, DOI: **10.1016/j.atmosenv.2015.10.032**.

47 K. Shukla, P. Kumar, G. S. Mann and M. Khare, Mapping Spatial Distribution of Particulate Matter Using Kriging and Inverse Distance Weighting at Supersites of Megacity Delhi, *Sustain. Cities Soc.*, 2020, **54**, 101997, DOI: **10.1016/j.scs.2019.101997**.

48 A. Hollingsworth, Objective Analysis for Numerical Weather Prediction, *Journal of the Meteorological Society of Japan. Ser. II*, 1986, **64A**, 11–59, DOI: **10.2151/jmsj1965.64A.0_11**.

49 K. Hayashi, K. Ono, M. Kajiura, S. Sudo, S. Yonemura, A. Fushimi, K. Saitoh, Y. Fujitani and K. Tanabe, Trace Gas and Particle Emissions from Open Burning of Three Cereal Crop Residues: Increase in Residue Moistness Enhances Emissions of Carbon Monoxide, Methane, and Particulate Organic Carbon, *Atmos. Environ.*, 2014, **95**, 36–44, DOI: **10.1016/j.atmosenv.2014.06.023**.

50 P. K. Nagar and M. Sharma, A Hybrid Model to Improve WRF-Chem Performance for Crop Burning Emissions of PM2.5 and Secondary Aerosols in North India, *Urban Clim.*, 2022, **41**, 101084, DOI: **10.1016/j.uclim.2022.101084**.

51 A. Awasthi, B. Sinha, H. Hakkim, S. Mishra, V. Mummidivarapu, G. Singh, S. D. Ghude, V. K. Soni, N. Nigam, V. Sinha and M. N. Rajeevan, Biomass-Burning Sources Control Ambient Particulate Matter, but Traffic and Industrial Sources Control Volatile Organic Compound (VOC) Emissions and Secondary-Pollutant

Formation during Extreme Pollution Events in Delhi, *Atmos. Chem. Phys.*, 2024, **24**(18), 10279–10304, DOI: **10.5194/acp-24-10279-2024**.

52 Y. Hao, J. Strähl, P. Khare, T. Cui, K. Schneider-Beltran, L. Qi, D. Wang, J. Top, M. Surdu, D. Bhattu, H. S. Bhowmik, P. Vats, P. Rai, V. Kumar, D. Ganguly, S. Szidat, G. Uzu, J.-L. Jaffrezo, R. Elazzouzi, N. Rastogi, J. Slowik, I. E. Haddad, S. N. Tripathi, A. S. H. Prévôt and K. R. Daellenbach, Transported Smoke from Crop Residue Burning as the Major Source of Organic Aerosol and Health Risks in Northern Indian Cities during Post-Monsoon, *Environ. Int.*, 2025, **202**, 109583, DOI: **10.1016/j.envint.2025.109583**.

53 P. Misra, S. Hayashida, M. Moriyama and H. Araki, Limitations of Interpreting Orbiting Satellite-Based Fire Detection for Crop Residue Burning: Has Agricultural Burning in North-West India Decreased in Recent Years?, *Int. J. Appl. Earth Obs. Geoinf.*, 2025, DOI: **10.2139/ssrn.5182780**.

© 2025 The Author(s). Published by the Royal Society of Chemistry

Environ. Sci.: Atmos., 2025, **5**, 1211–1229 | **1229**